remote sensing

MDPI

Review

A Systematic Review of Urban Flood Susceptibility Mapping: Remote Sensing, Machine Learning, and Other Modeling Approaches

Tania Islam [1], Ethiopia B. Zeleke [1], Mahmud Afroz [2] and Assefa M. Melesse [1,*]

[1] Department of Earth and Environment, Institute of Environment, Florida International University, Miami, FL 33199, USA; tisla015@fiu.edu (T.I.); ebisr001@fiu.edu (E.B.Z.)
[2] Department of Geosciences, University of Arkansas, Fayetteville, AR 72701, USA; mafroz@uark.edu
* Correspondence: melessea@fiu.edu

Abstract: Climate change has led to an increase in global temperature and frequent intense precipitation, resulting in a rise in severe and intense urban flooding worldwide. This growing threat is exacerbated by rapid urbanization, impervious surface expansion, and overwhelmed drainage systems, particularly in urban regions. As urban flooding becomes more catastrophic and causes significant environmental and property damage, there is an urgent need to understand and address urban flood susceptibility to mitigate future damage. This review aims to evaluate remote sensing datasets and key parameters influencing urban flood susceptibility and provide a comprehensive overview of the flood causative factors utilized in urban flood susceptibility mapping. This review also highlights the evolution of traditional, data-driven, big data, GISs (geographic information systems), and machine learning approaches and discusses the advantages and limitations of different urban flood mapping approaches. By evaluating the challenges associated with current flood mapping practices, this paper offers insights into future directions for improving urban flood management strategies. Understanding urban flood mapping approaches and identifying a foundation for developing more effective and resilient urban flood management practices will be beneficial for mitigating future urban flood damage.

Keywords: urban flooding; flood susceptibility mapping; GIS; remote sensing; machine learning

Academic Editor: Hatim Sharif

Received: 21 December 2024
Revised: 30 January 2025
Accepted: 31 January 2025
Published: 3 February 2025

Citation: Islam, T.; Zeleke, E.B.; Afroz, M.; Melesse, A.M. A Systematic Review of Urban Flood Susceptibility Mapping: Remote Sensing, Machine Learning, and Other Modeling Approaches. *Remote Sens.* **2025**, *17*, 524. https://doi.org/10.3390/rs17030524

1. Introduction

Flooding is one of the most catastrophic natural disasters worldwide, and it causes widespread damage to property and livelihoods [1]. Recent findings indicate that climate change notably contributes to flooding events by altering the intensity and frequency of rainfall patterns and decreasing the soil infiltration capacity [2,3]. Owing to global warming, the frequency and magnitude of extreme flood events are projected to increase, resulting in more substantial impacts on people and the economy than any other environmental disaster [4]. Research findings have also indicated that nearly 30% of losses from annual natural disasters are related to flooding [5]. A total of 2.23 million km square areas flooded around the world from 2000 to 2018 [6], and approximately 20–30 million people annually are affected by flooding [7]. According to a study finding, approximately two billion people will reside in flood-susceptible zones due to global warming and extreme weather events [8].

Urban flooding is one of the most expensive natural disasters on Earth due to climate change, altered rainfall events, rapid urbanization, and population growth [9–13]. Over the past few decades, land use and land cover patterns have undergone dramatic changes, such as a reduction in green spaces and a loss of wetlands, along with the expansion of built-up areas [14,15]. Settlement and built-up areas have led to an increase in impervious surfaces, which has led to increased surface runoff and strain on drainage systems during heavy rainfall [16–18]. Extensive population growth in urban regions has resulted in the exacerbation of urban flooding events and has emerged as a critical challenge on a global scale [16,19–22]. According to previous research, more than half of the world's population lives in urban regions [23,24], and areas with large populations experience urban heat island effects and relatively high aerosol loads, which lead to notable increases in precipitation [25,26], contributing to increased flood risk. By 2050, 65% of the world's population is expected to migrate to urban areas, resulting in an increase in commercial and economic growth [27]. The consequences of urban flooding are devastating, encompassing loss of life, infrastructure and property damage, economic setbacks, health risks, and environmental contamination in different regions worldwide [28–32]. This rapid urbanization also heightens the risk of urban flooding, making it crucial to better understand urban flood susceptibility mechanisms to support efforts in mitigating flood damage.

Flood susceptibility is commonly defined in the literature as the probability of a particular area experiencing flooding, influenced by environmental, topographic, and climatic factors [33]. Mapping flood susceptibility has increased in recent years, especially in urban regions due to the above mentioned climatic, and anthropogenic factors [34,35]. Flood susceptibility mapping is one of the most effective strategies for flood prevention and mitigation, as it identifies the most vulnerable areas and determines the likelihood of flooding [36,37]. It requires the integration of multiple data sources, including topographic, hydrologic, and meteorological data, and the selection of appropriate methodologies [38,39]. Identifying the appropriate method and the suitable resolution of the datasets and set of parameters ensures that these data sources are effectively integrated [40]. In addition, the accuracy and reliability of these maps require a thorough understanding of datasets, parameters, and methods [41–43].

Several studies have advanced flood susceptibility mapping by utilizing various flood causative factors and approaches [44]. For example, artificial neural networks and adaptive neuro-fuzzy inference systems (AN-FISs) have been applied to analyze factors such as elevation, slope, rainfall, land use, and proximity to rivers [45]. Other approaches, such as the analytic network process and weighted linear combinations, integrate factors including vegetation index, soil type, and lithology [46]. Recent reviews in flood susceptibility mapping research provide valuable information on the parameters and methods that shape current approaches [2]. Studies revealed a variety of flood susceptibility mapping (FSM) methods, with nearly 160 distinct approaches identified and parameter usage varying widely—from as few as five to over twenty in a single study [2]. Commonly used FSM approaches include multicriteria decision-making (MCDM), physical-based hydrological models, statistical techniques, advanced machine learning, and soft computing methods [2,47].

Despite these advancements, challeneges in optimizing model selection, parameter choices, and validation methodologies for FSM persist [48]. The field has witnessed a marked transition from traditional judgment-based approaches to data-driven techniques, reflecting an increasing reliance on big data and machine learning to enhance accuracy and predictive capabilities [2,49]. This evolution in FSM demonstrates the growing sophistication of available tools and methods while also highlighting the ongoing need to balance complexity with practical applicability. Additionally, while past studies have laid a strong foundation for understanding FSM, they often overlook the unique complexities of urban

environments. Unlike conventional settings, urban areas present distinctive challenges due to their varied features, unique drivers, and specific data requirements [50]. Directly applying traditional flood susceptibility mapping methods in urban areas introduces uncertainties in dataset selection, parameterization, and methodology. This gap raises critical questions about which approaches, parameters, and spatial datasets are most suitable for urban FSM. Addressing this need is essential, as urban flood susceptibility is shaped by unique geographical factors and requires careful consideration of method applicability and spatiotemporal resolution.

In recent years, there has been a dramatic increase in urban flood events globally, driven by climate change, rapid urbanization, and aging infrastructure [51–53]. While different studies have examined urban FSM, the literature remains fragmented across different methodological approaches, geographical contexts, and disciplinary perspectives. The unique contribution of this work is that it consolidates findings from diverse methodological approaches, compares the effectiveness of different assessment techniques, identifies consensuses and contradictions in the current understanding, and bridges gaps between academic research and practical applications. In addition, such studies can inform policy and practice, guide urban planning and zoning decisions, improve flood risk assessment methods, enhance emergency response strategies, and support infrastructure investment decisions. Therefore, the objective of this work is to provide a thorough and in-depth overview of urban FSM approaches, ranging from traditional methods to advanced machine learning and big data analytics, as well as to assess the effectiveness, advantages, and limitations of these diverse methodologies, which can provide valuable information for future urban FSM on a global scale. Additionally, this paper aims to evaluate commonly used remotely sensed datasets along with their suitability in different urban contexts and critically synthesize various flood causative parameters and how the same parameters may have varying effects depending on local geographic and environmental conditions. The global scope of this review is to provide a valuable understanding of and critical insight into the complexities involved in urban flood mapping, making it applicable to diverse urban contexts. Given the growing threats of urban flooding to life and infrastructure, this synthesis of current knowledge and methodological understanding aims to support more effective urban flood management practices and guide future research directions.

2. Materials and Methods

This study focuses on evaluating remotely sensed data and the various methods and parameters employed in urban FSM. The primary objective of this study is to provide a comprehensive analysis of how urban flood susceptibility is mapped and assessed across different regions. To achieve this goal, a detailed and extensive literature review was conducted, and inclusion criteria were carefully established to ensure the focused retrieval of relevant studies. The inclusion criteria were as follows:

- Articles must be peer reviewed;
- The study focus has to be urban flood susceptibility;
- Full-text articles must be available in English.

This review followed a step-by-step procedure, starting with a widespread literature search using specific keywords, followed by abstract screening to confirm the relevance of the research objectives. A targeted search strategy utilizing specific keywords related to urban FSM, such as “urban*”, “urban flooding”, “flood susceptibility”, and “urban flood susceptibility”, was implemented. An extensive literature search was conducted thoroughly via Google Scholar and the Web of Science core collection, and papers were identified. After that, a thorough abstract screening was also conducted to ensure the relevance of the study focus. We obtained 540 papers via keyword search. After the abstract

screening, 300 papers that did not necessarily focus on flood susceptibility in urban regions were excluded. Furthermore, full-text screening was conducted, and 120 papers were excluded because these articles did not necessarily fit our inclusion criteria. On the basis of these criteria, this review included 120 articles that focused on urban FSM and were published from 2012 to September 2024, ensuring that the review incorporated all the recent and relevant studies.

The methodology involved screening detailed information from selected studies, focusing on remote sensing data, flood influencing parameters, and methods employed in urban FSM worldwide. The analysis examined various flood causative factors and their importance, considering how they vary across diverse urban contexts, and identified future research directions. The step-by-step literature selection flowchart is given in Figure 1.

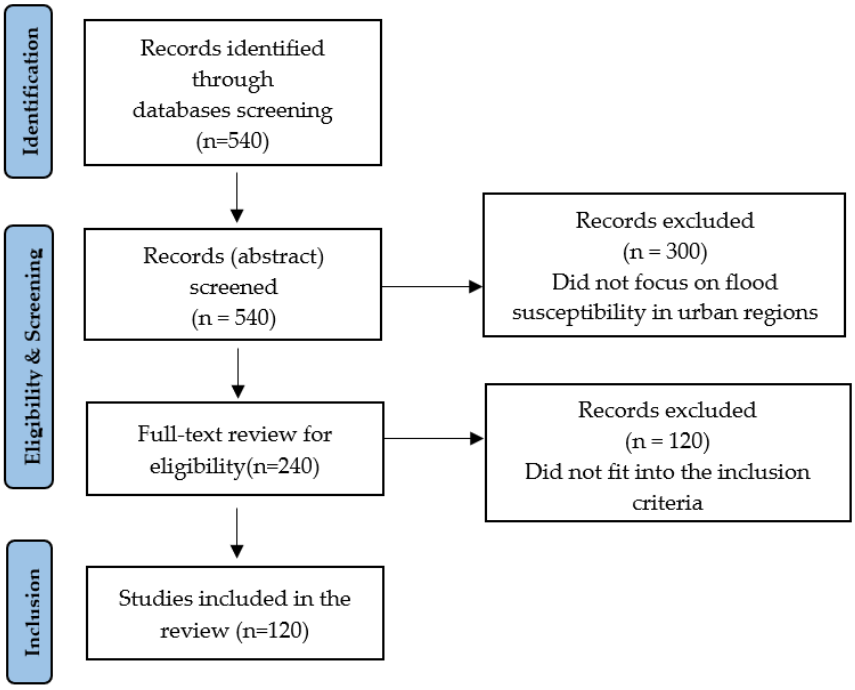

Figure 1. Literature selection flowchart.

An analysis of publication trends revealed a steady increase in urban FSM research since 2016, reflecting the growing recognition of flood risks in expanding urban environments under climate change [54]. This research growth is illustrated in Figure 2.

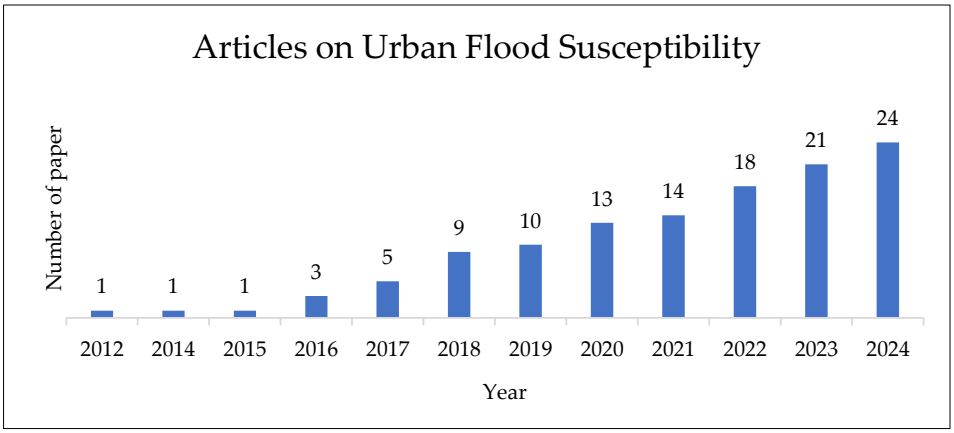

Figure 2. Articles related to urban FSM throughout the study period (2012–2024).

3. Data Used for Urban FSM

In recent years, the use of satellite-based remote sensing (RS) data has significantly advanced flood susceptibility mapping and assessment [55,56]. The availability of high-resolution datasets from missions such as Landsat, Sentinel [57], and Shuttle Radar Topography Mission (SRTM) has improved flood mapping by providing topographical, land cover, and surface water information. Accurate flood mapping and risk assessment rely heavily on digital elevation models (DEMs), which are used to determine flood depth by comparing terrain elevation with water levels [58]. Many studies utilize 30 m resolution DEMs (Table 1) due to their effective balance between spatial coverage and detail for large-scale flood mapping [59]. Some studies utilize Sentinel-1 SAR data (10 m) to extract flood zones for their atmospheric correction (spatial filtering) and cloud penetrating quality [60,61], as atmospheric correction helps reduce the noise of the raw Sentinel-1 SAR imagery [62,63]. This resolution is generally sufficient for identifying flood-prone areas and assessing potential impacts on a broad scale [64]. However, the selection of an appropriate spatial scale is critical, particularly in flat terrains and monsoon-prone regions [65]. In such areas, even minor errors in DEM data can lead to significant inaccuracies in estimating flood extent [66]. Thus, the precision of DEMs becomes crucial in these contexts to avoid misleading estimates of flood extent. Given these challenges, high-resolution data have become vital for reliable flood susceptibility mapping. Notable remotely sensed data that offer fine-scaled topographic estimates with reasonable accuracy include SAR (Synthetic Aperture Radar) images and LiDAR (Light Detecting and Ranging) sensor data, which are applicable to various urban (sparse vegetation) landforms and have the ability to detect flood depths [67,68]. While high-resolution DEMs offer improved detail and accuracy, factors such as cost, computational demand and accessibility can limit their availability and use [69]. Therefore, balancing the need for detailed and accurate data with practical considerations of cost (financial and computational) and accessibility remains a key aspect of DEM selection for flood susceptibility mapping.

Accurate flood mapping relies not only on detailed topographic data but also on precise precipitation measurements [70,71]. Remotely sensed precipitation data, derived from satellite observations, offer gridded rainfall and snow estimates, which are essential in areas with sparse gauges and remote locations [72]. Studies have most commonly utilized these precipitation products to estimate the spatial variability in the magnitude of precipitation [73] and, in some cases, to estimate the frequency and intensity of extreme rainfall events, thereby quantifying return periods relevant for flood mapping [60]. Long-term and uninterrupted records of satellite-derived precipitation data help quantify the likelihood of various flood risks across both space and time. Despite these advantages, satellite-derived precipitation data must be carefully integrated with ground-based observations to address potential biases [74]. High-resolution, low-latency, and long-term precipitation records, such as those provided by Climate Hazard Infrared Precipitation with Stations (CHIRPS), integrate gauge and satellite data to deliver more accurate and timely information [75]. This integrated approach allows researchers to contextualize recent extremes within a historical framework [75] and offers the ability to analyze the return periods of extreme precipitation events at various spatial scales, which are pivotal in flood susceptibility mapping and preparedness. This capability enhances the accuracy and relevance of flood susceptibility maps, thereby supporting more targeted and effective interventions in high-risk areas.

Land cover and land use data further enhance urban flood mapping. Land cover describes physical surface characteristics, whereas land use refers to the purpose of the land [76]. Remotely sensed datasets provide continuous information on both aspects that have been used to map flood susceptibility in numerous studies (Table 1). Satellite-driven

data through image classification are typically grouped into spectral classes on the basis of reflectance across multiple spectral bands, which are then assigned a specific land cover class. These classes, either pixel- or object-based [77,78], are then used to detect changes in land cover that may exacerbate flood risk, such as urban expansion or deforestation. In urban environments, where flood susceptibility is often highest, land cover data from sensors such as Sentinel–1 SAR- and Landsat-derived indices such as the normalized difference built-up index (NDBI) have been used to identify impervious surfaces that reduce infiltration and increase runoff. This is particularly relevant for areas where rapid urbanization alters natural hydrology, which contributes to increased flood susceptibility. Global land use and land cover datasets, such as those derived from Sentinel–2 (fine spatial resolution), Landsat 8 (moderate spatial resolution), and MODIS (coarse spatial resolution) data, have frequently been utilized to create spatially explicit flood maps that capture the impacts of various land cover types on flood risk. The range of spatial scales from these datasets offers the ability to detect land cover changes in rapidly urbanizing regions, as well as to perform large-scale flood risk assessments.

A summary of the varieties of remote sensing datasets that inform analyses of land use, precipitation, topography, and soil properties is presented in Table 1. This table outlines key remote sensing datasets utilized in the literature and details the respective resolutions and platforms or organizations from which the data were sourced.

Table 1. Summary of the remote sensing data used in the reviewed literature.

Variable	Dataset (Resolution Used)	Source/Provider/Platform
Land Use/Land Cover	Sentinel-2 (10 m) [23,60,79,80] MODIS (500 m) [9,81] Sentinel-1 [82] Landsat-8 OLI/TIRS (30 m) [40,83–98] GLOBELAND30 (30 m) [61,99–102] Land30 (30 m) [103] SinoLC-1, 2023 (1 m) [104]	ESRI Sentinel-2 land use/land cover downloader [23] Sentinel Scientific Hub [80] Coper–icus-ESA [82] Earthexplorer.gov [85] United States Geological Survey (USGS) [83] National Geomatics Center of China [99] GLOBE, Earth Science Data System [103] https://zenodo.org/records/8214871 (accessed on 30 January 2025) [104]
Precipitation	CGIS UR Rainfall * [23], Climate Hazard Infrared Precipitation with Station (CHIRPS) (0.05-degree) [105] Tropical Rainforest Measuring Mission (TRMM)—(0.25-degree) [79]	The Centre for Geographic Information Systems and Remote Sensing—CGIS-UR) [23] US Geological Survey Earth Resources Observation and Science Center [105], NASA [79]
Normalized Difference Vegetation Index (NDVI)	Landsat 8 (30 m) [60,61,86,99,104,106–108]	Google Earth Engine (GEE) [99]
Normalized Difference Built-up Index (NDBI)	Landsat TM/ETM (30 m) [93,109–111] Landsat 8 [104,105]	United States Geological Survey (USGS) [109]

Table 1. *Cont.*

Variable	Dataset (Resolution Used)	Source/Provider/Platform
Topography (DEM, DTM, DSM)	DTM * (1 m) [112,113] DEM * (10 m) [23,114] DEM * (5 m) [107] DEM * (30 m) [115] SRTM DEM (30 m) [60,61,82–85,88,90–92,94,99,101–103,116–121] SRTM DEM (90 m) [122,123] Open topography DEM (30 m) [80] LiDAR DTM (1 m) [124,125] Cartosat DEM (30 m) [126] ASTER GDEM (30 m) [40,79,81,93,96,98,100,109–111,127] Light Detecting and Ranging (LiDAR) (5 m) [128,129] Advanced Land Observing Satellite Phased Array Type L-band Synthetic Aperture Radar (ALOS PALSAR) (12.5 m) [128] ASTER DEM (27 m) [87] Topographical curves [36]	Authorative Topographic-Cartographic Information System (ATKIS) [112] Centre for Geographic Information System and remote sensing at the University of Rwanda [23] National Center of Geographic Information of Burundi [114] Department of Irrigation and Drainage (DID) Malaysia [107], The National Earth Observation Data Center (NODA) [113] Earthexplorer.gov [85] Global FABDEM (Forest and Buildings removed Copernicus DEM) [115] Open topography data archive [80] National Geospatial Intelligence Agency (NGA) [116] Earth Explorer USGS [79,82,87,99] Instituto de Planejamento Urbano de Florianópolis (IPUF) [36]
Soil properties (moisture, texture, type, depth, class)	Soil texture layer [23] Soil Moisture Active Passive (SMAP) satellite [130] SoilGrids (250 m) [81]	Rwanda Soil Information Service Project (RwaSIS) [23] NASA [130] ISRIC World Soil Information [81]
Urban flooding area/sprawl area/flood inventory map	Sentinel 1 SAR (10 m) [61,131], landsat global dataset of human builtup and settlement e–tent—HBASE (30 m) [81] Landsat estimated global surface water (30 m) [60] IKONOS (1 m) [28]	GEE [61], Socio Economic Data and Application Center (SEDAC), Global Land survery derived Landsat imagery [81] ESA/Copernicus Global Surface Water Explorer (GSWE) [60]

* Dataset sourced from national institutions.

4. Parameters Used for Urban FSM

To evaluate urban flood susceptibility, it is important to understand the relationships between flood causative parameters and flood events [2,132,133]. Different studies have shown that urban flood susceptibility is a complex phenomenon because it depends on topographical, hydrological, and geographical contributing factors [10,108]. The selection of parameters for urban FSM is challenging as there are no specific guidelines for parameter selection [39,134]. Rather, the selection of flood causative factors often depends on the physical and natural characteristics of the study area, the availability of datasets, and the granularity of the desired outcome [135,136]. These parameters can be used to determine existing conditions, compare various circumstances in different locations, and provide future recommendations for understanding trends or future impacts [48,137]. In addition, parameters play important roles in the accuracy and reliability of urban FSM as they contain important information regarding the physical characteristics of the study area [138,139]. For example, topography and slope are essential for evaluating water accumulation and runoff dynamics, land use patterns highlight the spread of impervious surfaces, and geological features provide insights into water absorption and retention capacities during heavy rainfall [2]. Each influencing parameter offers unique and valuable information that can help with accurate and detailed flood susceptibility mapping in urban regions. Therefore, selecting the appropriate parameter that accurately represents the flooding scenario is crucial in urban FSM [140].

Researchers have used a range of flood causative parameters to map urban flood susceptibility around the world. We divided the parameters into two different groups, namely primary and derivative parameters. The primary flood causative parameters, along with their commonly used synonyms, are summarized in Figure 3 and include the following: elevation (altitude or drop raster), land use and land cover, rainfall (precipitation), proximity to rivers, channels, drainage systems, or streams, soil properties (group, texture, permeability, or hydraulic conductivity), geology (lithology or hydrolithology), distance from roads or streets, proximity to stormwater drainage systems, sewers, or hydrographic networks, groundwater level or depth, locations of drainage pump stations or stormwater outfalls, proximity to dry drainage areas or depressions, wetland degradation, presence of rainwater retention devices, swampy areas, and infrastructure density (e.g., roads, buildings, bus stops). Below is a detailed summary of these key parameters.

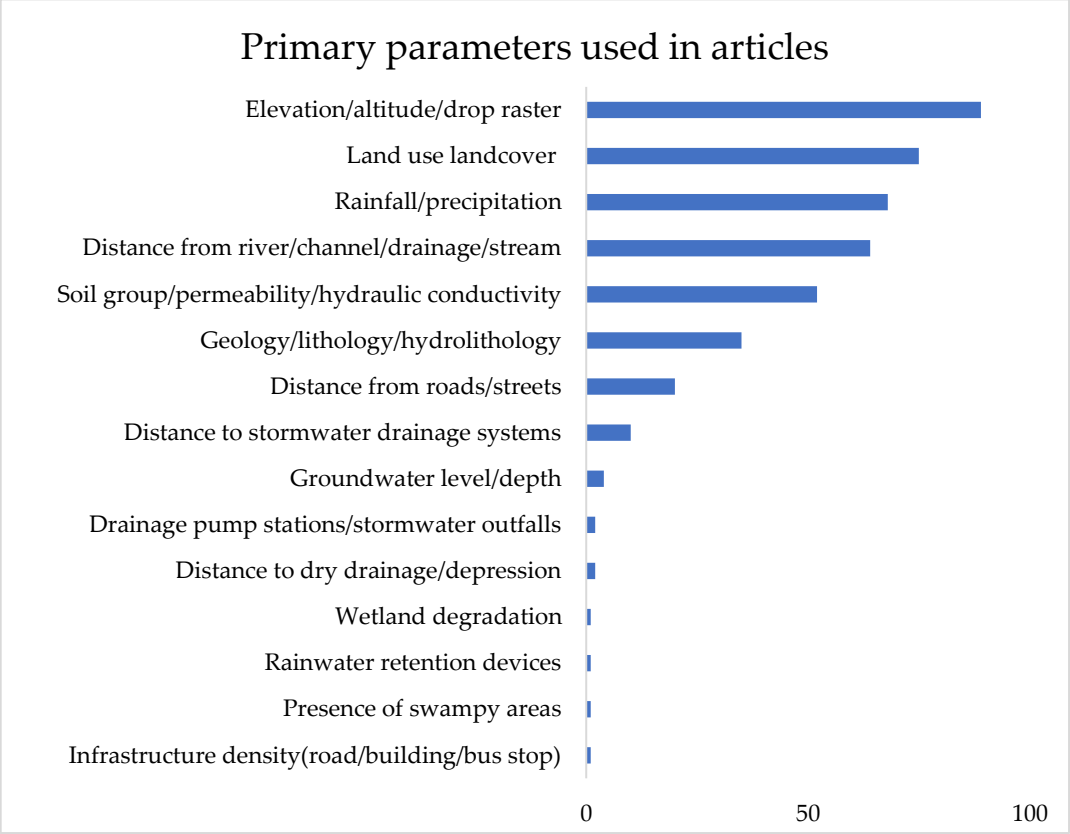

Figure 3. Primary parameters used in urban FSM articles.

Elevation/altitude/drop raster: Elevation is a critical factor in flood susceptibility, as it governs the flow of water. Areas at higher elevations typically experience rapid water movement, which reduces absorption time and increases the risk of flooding downstream. Conversely, lower elevations are more prone to water accumulation and flooding [141–143]. Elevation data, often derived from digital elevation models (DEMs), plays an integral role in flood modeling by defining topography and guiding water flow analysis [144–147]. Drop raster, representing altitude or elevation on a grid-cell basis, further aid in understanding flow direction and flood patterns [148,149]. Proper drainage planning is essential for settlements across various elevations to mitigate flood risks [150–152].

Land use and land cover: Land use land cover is one of the most important flood conditioning factors affecting urban flood susceptibility [153,154]. Land use land cover processes caused by both manmade and natural factors have significant effects on flooding. Built-up and settlement areas are positively associated with urban flooding. Impervious

surface areas are responsible for surface runoff and lead to flooding. Additionally, if the land is closer to the water body, those areas have a high potential for flooding [155,156]. On the other hand, vegetated areas have a negative correlation with flood susceptibility because soil has a greater absorption capacity than urban areas. Vegetated and green agricultural areas improve the infiltration rate of water into the soil during intense rain events, thereby mitigating the risk of flooding. Therefore, urban areas closer to agricultural land are less prone to flooding.

Rainfall/precipitation: Rainfall characteristics, including intensity, duration, and volume, are fundamental drivers of urban flooding [148,150,154,157]. Heavy rainfall over short durations saturates soil quickly, while prolonged events on impervious surfaces exacerbate runoff [158,159]. When stormwater drainage systems reach capacity, streets and infrastructure become inundated, leading to widespread flooding [160–162]. Effective urban flood management requires detailed analysis of rainfall patterns and stormwater system capacities.

Distance from river/channel/drainage/stream: Proximity to rivers, channels, and drainage networks is a key determinant of flood risk. Areas near water bodies, such as lakes, rivers, and canals, are more susceptible to inundation during heavy rainfall events, particularly when these systems exceed their capacity [121,157,163,164]. Settlements closer to water bodies are at greater risk due to overflow and runoff, underscoring the importance of maintaining buffer zones in urban planning [144,146,165,166].

Soil group/texture/permeability/hydraulic conductivity: Soil hydrology determines the surface runoff scenario, and it is an important parameter for determining flood occurrence [141,167,168]. It occurs when the soil is either saturated or exceeds its capacity to absorb water in the ground and overflow [117,146,162]. Some soils for example, sandy soils have relatively high infiltration rates and can absorb water quickly resulting in relatively low surface runoff and less flooding [23,84,126,169]. Conversely, some soils such as clay soils have lower infiltration rates resulting in more surface runoff and higher flooding risk [170]. Urban expansion leads to the expansion of impervious surfaces, and surface runoff is positively correlated with this process [166,171]. The impermeable surface areas are positively correlated with flooding. In urban areas, impervious surfaces behave as active runoff sources and can be flooded with a short amount of rainfall [172]. Erosivity plays a crucial role in flood mechanisms. High erosivity results in rainfall with a greater potential to dislodge soil particles [18]. In urban regions, more sediment enters drainage systems and waterways, clogging stormwater systems and exacerbating flood risk [173].

Geology/lithology/hydrolithology: Geology/lithology plays a crucial role in urban flood mapping [151,174]. If the surface is permeable and contains more pore spaces, rainwater can directly pass through the porous surface to the ground [142,152]. Impermeable surface areas are less capable of water infiltration and more prone to flooding [161,167,168]. Urban areas covered with impervious surfaces have very low permeability during heavy rainfall, which results in flooding [146,156].

Distance from roads/streets: Distance from roads plays a vital role in flood occurrence [105,112,175]. Roads and streets are cemented, and concrete materials and impervious surfaces are responsible for surface runoff [83,160]. Impervious surfaces create obstacles for water to percolate through the soil. The greater the impervious surface area is, the greater the risk of flooding [129,176,177]. Urban areas contain streets, sidewalks, and major roads, which are responsible for water accumulation during heavy rainfall [88,93].

Distance to stormwater drainage systems/sewers/hydrographic networks: Settlements and built-up areas near well-maintained stormwater drainage channels/sewers mitigate urban flood risk by quickly releasing rainwater [79,122,178]. Built-up areas far

from stormwater drainage areas experience faster water accumulation and greater surface runoff and urban flooding [129,173].

Groundwater level/depth: The greater the groundwater table is, the less space there is for water absorption [117]. This means that the soil is already saturated with water. Therefore, when it rains, it does not have a greater capacity to absorb water [148]. This results in greater surface runoff during heavy rainfall, which contributes to urban flooding.

Drainage pump stations/stormwater outfalls: In urban areas, drainage pump stations/stormwater outfalls play an important role in managing excessive rainwater by passing through directly to the ground [103]. Drainage pump stations contain pumps/lines that can transport large volumes of stormwater in times of heavy rainfall in urban areas. The greater the number of stormwater outlets, the lower the chances for water accumulation [179]. Sometimes, urban areas are largely crowded with buildings, roads, and sidewalks and less permeable surfaces, and drainage pump stations help release rainwater to the ground and reduce the risk of flooding.

Distance to dry drainage/depression: Dry drainage/depression mostly works as a natural water reservoir during heavy rainfall events [125]. Urban areas located near dry drainage areas have lower chances of heavy runoff. A short distance from dry drainage areas leads to rapid and efficient drainage that helps mitigate the risk of urban flooding by removing excess water. Settlements and built-up areas closer to depressions, such as any low-lying area, may experience rapid flooding to a greater extent than those farther away [104].

Wetland degradation: In urban regions, wetlands work as natural reservoirs, absorbing excessive amounts of water during heavy rainfall [86]. Therefore, wetland degradation has significant effects on flooding by reducing the natural absorption capacity, and exacerbating surface runoff and flood risk. Satellite imagery and aerial photography can be used to incorporate wetland data in urban FSM.

Rainwater retention devices: Urban areas are covered with impervious surfaces such as concrete, asphalt, and bricks that block rainwater from passing through the ground and accelerating surface runoff. Rainwater retention devices allow rainwater to slowly infiltrate the ground and mitigate urban flooding [60]. This helps reduce surface runoff, delays peak flow, and controls localized flooding.

Presence of swampy areas: Swampy areas work as reservoirs and can store large volumes of water during heavy rainfall events in urban region [84]. These areas are capable of absorbing excessive water during heavy downpours. Therefore, they help reduce surface runoff and the risk of flooding in adjacent urban areas. Vegetation indices such as normalized difference vegetation indices or soil survey data can be used to incorporate the presence of swampy areas in urban FSM.

Infrastructure density (road/building/bus stop): Infrastructures such as roads, buildings, and bus stops reduce the capacity of the soil to absorb rainwater, which intensifies surface runoff [129]. Therefore, areas closer to settlements and infrastructures are highly susceptible to urban flooding. Infrastructure density data can be gathered from land use land cover data and the normalized difference built-up index for urban FSM analysis.

The derivative parameters include slope/terrain slope, topographic wetness index, drainage density, curvature/profile curvature/plan curvature, aspect, normalized difference vegetation index, stream power index, flow accumulation, terrain ruggedness index, normalized difference built-up index, runoff, slope length factor, modified Fournier index, convergence index, coefficient of compactness, sediment transport index/susceptibility to production of sediment, concentration time, peak flood discharge, and Gravelius coefficient. The derivative parameters are listed in Figure 4. A summary of derivative parameters is described below.

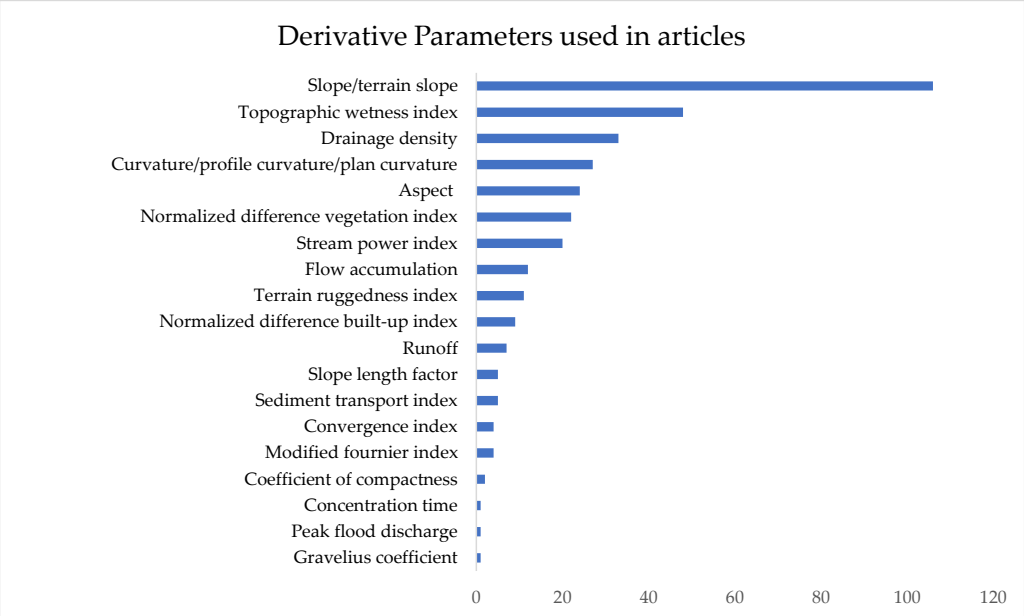

Figure 4. Derivative parameters used in urban FSM articles.

Slope/terrain slope: Slope plays an important role in mapping urban flood susceptibility and researchers have used this parameter to map urban flood susceptibility [175,179]. It is proportional to surface runoff and influences flooding. Slope affects the infiltration rate and speed of surface runoff [157,163,178,180,181]. It is measured by the angle between the terrain and horizontal data, and gravity influences the generation of surface runoff and its speed [159,173,176,182,183]. Slope in urban regions have a direct impact on flood dynamics by influencing water flow and accumulation patterns [158,177,184,185].

- **Flat areas:** In flat regions, water tends to accumulate over time, which leads to prolonged flooding. Therefore, gentle slopes and flat areas are more susceptible to flooding [160–162]. A slope of 0–5% is considered a flat region.
- **Gentle slope:** In gentle slope areas, water flows more slowly than steep slopes. However, water may accumulate more easily because of ponding and inadequate drainage systems [171,174,186]. A slope of 5–15% is considered gentle slope.
- **Steep slope:** Steep slopes increase the surface runoff process and reduce the available time for the soil to absorb water [187–189]. Water travels downhill rapidly, which reduces the infiltration rate. Urban regions at the bottom of steep slopes are highly susceptible to urban flooding because they receive high volumes of water in a short period of time [166,167,169,190]. More than 15% slope is considered steep slope.

Topographic wetness index: The topographic wetness index (TWI) is a geomorphometric factor used to evaluate runoff in flood susceptibility mapping [106,121,152]. It determines the water-saturated areas and the spatial distribution of water on the surface and underground [168,183]. It is a key parameter for understanding the spatial distribution of water on the surface and underground [142,146,176]. It can be calculated via the following equation:

$$TWI = Ln\ (A_s / \tan \beta) \quad (1)$$

Here, A_s represents the upslope contributing area and tan β represents the slope at that point. High TWI values represent favorable areas for water accumulation and susceptibility to flooding.

Drainage density: Drainage density influences surface runoff and affects urban flooding [105,118,191]. A higher drainage density leads to shorter concentration times

and a greater risk of flooding [118,141,145,162,187]. Conversely, a lower drainage density leads to a lower probability of flooding [151,154,167,189].

Curvature/profile curvature/plan curvature: Curvatures play an important role in identifying areas that are prone to water accumulation as well as urban flooding [86,162]. Curvature affects the direction and velocity of surface runoff [152,184,186]. Profile curvature refers to the downward direction of the slope and the probability of flooding is greater on concave terrain [107,176]. The profile curvature affects the speed and concentration of water flow [99,182]. Plan curvature refers to the horizontal curvature perpendicular to the direction of the maximum slope. Negative curvature refers to concavity, positive curvature refers to convexity, and zero curvature refers to plane [141,143]. Negative curvatures are more prone to surface runoff and flooding [99].

Aspect: Soil humidity and flow direction are influenced by aspect [141]. Therefore, aspect is considered an important parameter for urban flood occurrence [184]. Aspect affects the direction of water flow in any landscape, [114,119,124,160]. For example, slopes facing certain directions influence water movement either slowly or rapidly when other factors, such as topography, soil hydrology, and land use are considered [19,83,91,176].

Normalized difference vegetation index: The normalized difference vegetation index (NDVI) affects the infiltration rate and surface runoff [106,144,188]. The NDVI is used to understand vegetation density and health [95,108,185]. Healthy vegetation is able to absorb rainwater, help reduce runoff and mitigate urban flooding [97,131,159]. Higher NDVI values indicate dense vegetation, which helps increase water infiltration and decreases flooding [160,170,174].

Stream power index: The stream power index (SPI) is positively correlated with flood susceptibility [79,142]. It represents the erosive capacity of water movement [83,97,102]. The SPI determines the flow strength and corrosive effect of water [11,154]. Higher SPI values indicate greater erosive power and are more susceptible to urban flooding [144,174].

Flow accumulation: Flow accumulation refers to a large volume of water flowing toward a specific area [169,186]. Urban areas are covered with many impervious surfaces, which can result in greater water pooling and increased risk of flooding [115,149,154].

Terrain ruggedness index: The terrain ruggedness index (TRI) determines the ruggedness or smoothness of a landscape [83,173]. The TRI is positively correlated with flooding risk [102,171]. A rugged terrain with a relatively high TRI indicates varied elevations and slope angles, which can create complex and multiple flow channels for surface runoff and increase flood risk [154,180]. Smoother terrain with a low TRI indicates less varied elevation differences and slower runoff, which helps mitigate flood risk [19].

Normalized difference built-up index: The normalized difference built-up index (NDBI) helps to identify the extent of impervious surface areas such as concrete, asphalt and buildings. Impervious surface areas work as obstacles to stormwater infiltration, leading to increased surface runoff and urban flooding [191]. By analyzing the NDBI, urban planners can identify areas with high runoff potential [110,192]. Settlements and built-up areas with high NDBI values are more likely to experience significant runoff, which can overwhelm drainage systems and contribute to urban flooding [109,111,147].

Runoff: Surface runoff is a crucial factor in urban FSM [81,129]. In urban areas, impervious surfaces such as buildings, roads, sidewalks, and pavements prevent water from infiltrating the ground. Surface runoff influences the severity and magnitude of urban flooding [87,146].

Slope length factor: The slope length factor affects the volume, speed, and erosive potential of surface runoff [99]. A longer slope allows more surface area for water accumulation during heavy rainfall [184]. This results in greater surface runoff and greater

potential for flooding. Runoff from longer slope lengths can cause heavy flooding in urban regions [10].

Sediment transport index: The sediment transport index (STI) refers to sediment movement in a landscape [168]. A higher STI results in greater sediment transport and greater erosion during heavy rainfall [102,107]. As a result, more sediment can be transported into rivers and streams, increasing flood risk. A lower STI indicates lower sediment transport and less soil erosion which helps to reduce flood risk in urban areas [60]. Sediment production and transport can alter urban drainage systems. High sediment production results in the accumulation of sediment in storm drains, canals, and other drainage infrastructures near urban regions. When drainage systems become clogged, their ability to release stormwater away from urban regions is compromised, leading to increased surface runoff and flooding [60]. Hydrological models such as the stormwater management model (SWMM) or the Hydrologic Engineering Center's Hydrologic Modeling System (HEC-HMS) can be utilized to simulate sediment transport.

Convergence index: The convergence index is positively correlated with flooding [180]. A higher convergence index leads to greater water accumulation and rapid surface runoff [80]. Areas with divergent flows are less likely to experience water accumulation. Therefore, lower surface runoff leads to lower flooding risk [182]. The convergence index can be calculated by combining flow accumulation with the slope or curvature of the terrain and can be employed in urban FSM.

Modified fournier index: The modified Fournier index refers to the evaluation of the erosive potential of rainfall [121]. It represents the ratio between the average monthly and average annual rainfall. It is used to determine the effects of extreme rainfall events on soil erosivity [11,180].

Coefficient of compactness: The coefficient of compactness affects the extent of impervious surfaces in an area [164]. Areas with higher coefficients of compactness lead to a greater distribution of impervious surfaces such as roads, bridges, pavements, buildings, and compact areas [60]. Areas that have higher compactness coefficients are more prone to rapid runoff and urban flooding.

Concentration time: Concentration time refers to the time it takes for water to travel from the farthest point to a specific point in a watershed [81]. In urban areas, a shorter concentration time can lead to a greater risk of water accumulation and severe flooding.

Peak flood discharge: Drainage systems in urban areas depend on how efficiently excessive rainwater can be discharged [81]. They are usually designed to absorb typical rainfall events. High peak discharge can sometimes exceed capacity and lead to rapid water accumulation and urban flooding. The peak flood discharge can be calculated by multiplying the runoff coefficient, rainfall intensity and drainage area of the watershed for urban FSM.

Gravelius coefficient: The Gravelius coefficient refers to the shape of a drainage basin. A low Gravelius coefficient indicates a basin with a more circular shape where the runoff concentration time is shorter. This results in higher discharge in a fleeting period and increases the flooding risk [87]. A higher Gravelius coefficient indicates a basin with an elongated shape where the runoff concentration time is longer. It allows time for slow discharge and reduces the risk of immediate flooding. The Gravelius coefficient can be calculated by measuring the perimeter and area of a polygon and can be utilized in urban FSM.

5. Methods Used in Urban Flood Susceptibility Mapping

Researchers have proposed various methods for urban FSM, and these methods differ from one another in terms of data availability, expert opinions, and ease of

application [193,194]. While the literature highlights diverse techniques, certain methods tend to be more effective in urban FSM depending on the regional context and specific study requirements [195,196]. For example, in areas where historical flood data are scarce, machine learning models are likely not a suitable option, as large datasets are needed to train the model [73,104]. Physically based hydrological models consider detailed data and significant computational resources, whereas statistical methods and soft computing techniques offer more straightforward implementations with varying accuracy and precision depending on various flood conditioning factors being analyzed. Therefore, the choice of method often depends on the characteristics of the study area, specific objectives, data availability, and accuracy required for urban FSM. Despite this effectiveness, there is no widespread consensus among scientists that these frequently used methods are superior to others. Each method has its strengths and limitations, making the selection highly context-dependent. Different approaches that have been used in urban FSM are listed in Figure 5.

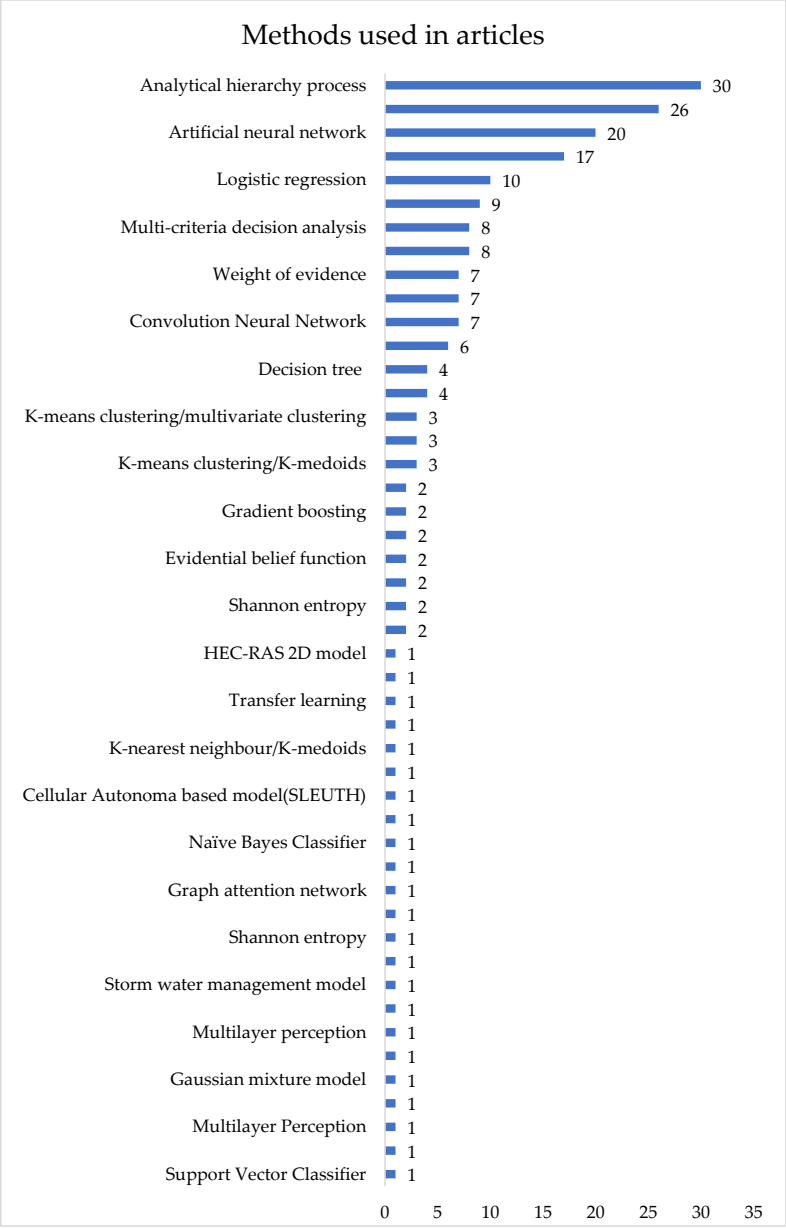

Figure 5. Urban FSM methods used in the articles.

5.1. Frequently Used Methods in Urban FSM

The most frequently used approaches include the analytic hierarchy process (AHP) [90,152,188], frequency ratio (FR) [162,167,197,198], logistic regression (LR) [161,199], weights of evidence (WoE) [143,200], Shannon's entropy (SE) [18], certainty factor (CF), multicriteria decision analysis (MCDA) [85,116,141,160,201], and fuzzy logic AHP [101,162,185–187,189,200,202,203]. In addition to these approaches, researchers have also most frequently utilized various physically based hydrological models, statistical methods, weighted overlays, and different soft computing approaches [183,204,205]. Researchers have also utilized a combination of 2-3 approaches to understand and evaluate the level of urban flood susceptibility [206]. In urban FSM, pairwise comparison matrix methods such as the AHP have often been used [60,118,171] and are highly preferred for more accurate urban FSM [13]. The AHP was developed by Saaty [207] and has been widely used for addressing complex environmental problems [171]. The AHP and modified AHP [125] are useful for identifying logical consistencies, building a single evaluation index by collecting information from different indicators [36,173,208]. They are highly flexible, easy to use, and widely employed in flood susceptibility parameters by researchers [84,85,108]. One of the major advantages of AHP is that it can integrate both qualitative and quantitative factors into the decision-making process [127]. This approach is also applicable from an individual and collective perspective and is suitable for local and regional susceptibility studies [60]. The AHP is considered a simple, cost-effective, and understandable approach for facilitating urban FSM and a powerful technique to support multicriteria decision-making [23,80,117,126]. Urban FSM involves the use of different flood conditioning factors, and GISs (geographic information systems) and RS (remote sensing) are considered effective tools for dataset extraction [88,166,173]. Researchers have also widely used geographic information systems (GISs) for determining flood conditioning factors in urban FSM datasets [169,172,209–211]. Over the years, GISs have been widely applied in hazard preparedness and decision-making processes [38,113,170,212]. Weighted overlay and weighted sum are also effective tools in GIS for urban FSM [13,23,114,126,127] where they combine various flood causative factors, assign different weights to each variable on the basis of their relative importance, and overlay or sum them to produce a flood susceptibility map. One of the major advantages of a weighted overlay is that it allows for and integrates both qualitative and quantitative variables in a single layer [23]. Researchers have frequently combined the AHP and weighted overlay method to map urban flood susceptibility [126,127,131]. Multicriteria decision analysis (MCDA) approaches are widely used in urban FSM [87,144] and provide a robust collection of technical procedures for designing, and evaluating alternative decision-making methods [213]. MCDA is a widely used method that helps researchers make effective decisions according to problems and factors. However, MCDA methods mostly rely on expert opinion to evaluate multiple criteria and provide subjective results [151].

The assessment of urban FSM involves univariate or multivariate models, including hydrological, statistical, and machine learning approaches [89,214]. Machine learning methods have demonstrated higher percentage of accuracy in effectively predicting urban flood-susceptible regions [215]. These methods such as fuzzy logic, genetic algorithms, and artificial neural networks are tolerant of ambiguity, fuzziness, and partial accuracy [87,95,150,174]. These approaches complement each other, instead of competing with each other, and can be utilized together to solve complex environmental problems [216,217]. The most frequently used machine learning methods include unsupervised clustering algorithms and supervised classification algorithms [182,218,219]. The supervised classification algorithm automatically evaluates and learns the associa-

tions between conditioning factors and associated labels and identifies flood-susceptible areas [220,221].

Studies prefer support vector machines, random forests, and artificial neural networks in urban FSM over other approaches because of their higher accuracy and certain advantages [21,153,222–225]. Support vector machines are among the most popular supervised learning algorithms and have received widespread attention because of their excellent performance in urban FSM [103,109,111]. Support vector machines generally require fewer training samples to achieve good performance compared to artificial neural network and different studies reported accuracy between 82–96%.

Random forest (RF) is a machine learning tool based on multiple decision trees and is capable of solving classification and regression problems [124,145,156]. RF trains random samples of data independently to derive weak models, and the average predictions from these weak models produce more accurate results [73,83,100,226]. RF avoids overfitting and can handle missing values during training [223].

Artificial neural networks are deep learning methods composed of an input layer, one or more hidden layers and an output layer [153,154]. A multilayered neural network is also a deep learning approach with multiple ANN input and output layers that can capture intricate patterns and are effective for urban FSM [130,148,227]. One of the advantages of this approach includes learning complex patterns by analyzing diverse data. Multilayer perception is also a type of artificial neural network approach that is effective at capturing complex relationship between multiple flood related parameters; however, careful tuning is needed to avoid overfitting spatial datasets [61]. Researchers have also utilized Shannon entropy (SE) to understand the correlation between flood contributing factors and flood events [40]. Researchers have utilized the gray wolf optimizer and bat optimizer to analyze urban FSM [181]; these optimizers utilize animal behavior to solve complex urban flooding problems. In [228], an autoregressive integrated moving average (ARIMA) approach was utilized to analyze the urban FSM in Anambra, Nigeria [228]. This approach is helpful in analyzing and predicting hydrological data such as rainfall and river discharge data for assessing future urban flood susceptibility. Researchers have also utilized urban deployment models with cellular automata via SLEUTH software. This approach aims to model and predict urban growth. SLEUTH stands for slope, land use, exclusion (building prohibition areas), urbanization, transportation, and hill shade, which are key factors in the model [127].

5.2. Methods by Sample Size

Urban FSM has evolved over time from traditional expert opinions to statistical, soft computing, big data, and machine learning methods [229,230]. The complex characteristics of urban flooding have led researchers to utilize machine learning heuristic approaches [92], as these approaches are capable of solving uncertain and complex real-life problems [231–233]. In addition, these methods have also demonstrated excellent performance in urban FSM [99,105,110,112,119]. However, these supervised model performances are largely determined by the sample size used for training. As the sample size for training increases, the model performance improves proportionally [234].

Researchers utilize historical flood data to train these machine learning models as these methods depend exclusively on sample size and input data. For example, support vector machines (SVMs) and convolutional neural networks (CNNs) are popular for classification in urban FSM, and this approach has frequently been used in spatial image processing fields and different prediction problems because of its feature extraction ability and excellent learning capacity [112,191]. Both SVMs and CNNs demonstrate better performance in urban FSM and the differences between their performances are minor [103]. CNNs do not

require manual feature extraction; rather, they use algebra to identify patterns to increase computational demand [157]. Frequency ratio approaches are also popular methods for urban FSM; however, large datasets are required to train such models [142,146,155]. In some urban regions, historical flood points are difficult to acquire and FR is not a good option for these areas.

5.3. Methods by Weighting

In urban FSM, the weighting of flood conditioning factors is crucial, and different methods can be utilized to assign weights to these factors [108,211,235,236]. Weights play an important role in urban FSM for evaluating results as they quantify the relative importance of different factors. The most common methods for developing weights are the analytical hierarchy process (AHP) [160], the entropy method (EM), and the maximal information coefficient (MIC). One of the limitations of using AHP is its high subjectivity, as it utilizes expert opinion and knowledge [237,238]. Conversely, the entropy method relies solely on objective data while considering the relationships among indicators [99]. The weighting utilized by the MIC can be sensitive depending on the distribution of the data. Unevenly distributed data can heavily affect the weights and the final outcome. Fuzzy logic can also be utilized to assign weights in urban FSM and it allows for more precise weighting compared with traditional binary classification. The fuzzy gamma operator is also an effective approach in urban FSM where flood causative factors can be assigned values between 0 and 1 [79].

5.4. Methods Based on Problem Type and Output Goals

The urban FSM output can vary depending on data availability and model selection. Bivariate statistical models are also effective in urban FSM, and they calculate the probability of flooding on the basis of each factor independently [28,91,143]. For example, logistic regression (LR) is a statistical approach for binary classification, and researchers have used LR for urban FSM [86,93,110,155]. This method is able to predict the likelihood of flooding in different regions on the basis of various flood conditioning factors. The outcome yields a probability score that indicates the likelihood of a particular area being susceptible to flooding or not. Similarly, the naïve Bayes classifier (NBS) is a probabilistic classification algorithm that relies on the Bayes theorem [92]. NBSs are particularly useful for analyzing complex datasets for urban FSM and predicting the likelihood of flooding in different urban regions [147]. Positive and background learning with constraints (PBLC) is a machine learning approach that helps distinguish between flood-prone areas and non-flood-prone areas in urban FSM [99]. On the other hand, Gaussian mixture model (GMM) clustering is a statistical tool that can be employed to understand urban FSM [179]. This model analyzes spatial data related to rainfall, elevation, land use, and drainage systems. By grouping areas with similar characteristics, the Gaussian mixture model can help identify flood susceptibility zones that are at greater risk. A decision tree is an ML model that can effectively solve classification and regression problems and can handle complex datasets [73]. Researchers have also used decision trees in urban FSM, and the benefits of decision trees include the fact that this approach can handle complex multidimensional datasets and is able to identify homogenous clusters with various susceptibility levels. K-means clustering is an effective approach for urban FSM, as it is also able to identify clusters of highly flood-susceptible zones on the basis of topographic and hydrologic data [179,182]. Similarly, kernel density has also demonstrated excellent performance in identifying flooding hotspots, particularly in dense urban settings [163].

5.5. Modeling Techniques for Regions with Sparse Data Availability

Physically based hydrological models are used robustly in urban FSM. Physically based hydrological models such as the SWAT (Soil and Water Assessment Tool) model can simulate hydrological processes such as rainfall–runoff, evapotranspiration, and channel flow. Studies also utilized MODFLOW (modular three-dimensional finite-difference ground-water flow model) to integrate surface and subsurface hydrology for mapping flood susceptibility. One-dimensional HEC-RAS models and two-dimensional TELEMAC-2D and RMA2 models are often used by researchers [116]. These models are effective in providing detailed simulations of flood scenarios and capturing the complexity of precipitation, infiltration, and surface runoff in urban regions. However, fieldwork and computational resources are required for data collection. In addition, in some regions, the scarcity of flood inventory data is a major problem when mapping urban flood susceptibility. Urban flood-prone areas are often dispersed where hydrological monitoring stations are scarce and high spatial resolution data may be missing [239]. These scenarios pose challenges in mapping urban flood susceptibility in those regions. Researchers have employed graph attention networks (GATs) to overcome this problem [191]. GATs utilize nodes and edges to represent spatial units and relative spatial relationships only via basic flood conditioning factors [191]. A graph attention network is a type of neural network algorithm and one of the advantages of this approach is that it can model complex spatial relationships and interactions among various geographic, topographic, and environmental factors [191]. In addition, researchers have coupled the physically based variable parameter Muskingum stage-routing (VPMS) module with the popular storm water management model (SWMM) to analyze urban pluvial flooding in urban and peri-urban areas where hydrological data and discharge information are limited [82,240]. Researchers have also utilized the transfer learning approach in urban FSM; in this approach, one task is reused as the starting point for a model on a second, related task [175]. Transfer learning can be a powerful machine learning tool in urban FSM in regions with similar topographic characteristics, especially where data availability is limited. This approach helps improve the deep learning model by transferring knowledge from a pretrained model that has already been trained on a large dataset in terms of urban FSM [175].

5.6. Methods Used to Improve Model Performance

Different heuristic approaches have been proposed by researchers to analyze urban flood susceptibility, and among these, soft computing approaches are designed with numerical intelligence that can modify the analysis environment and learn to produce better outcomes. For example, researchers have utilized boosted regression trees (BRTs), which combine multiple decision trees to improve model performance and accuracy [89,148]. BRTs are useful for urban FSM because they can effectively integrate remote sensing and GIS data to increase the mapping precision [184]. The evidential belief function, known as the Dempster–Shafer theory, is particularly useful in handling the uncertainty and imprecision of urban flooding problems [10,79]. Support vector classifiers (SVCs) can handle nonlinear data efficiently and demonstrate high accuracy in urban FSM [61].

Researchers have also utilized the adaptive boosting (AdaBoost) classifier for urban FSM in different regions [159]. The AdaBoost classifier is an ensemble ML model that combines various weak learners into a strong learner and focuses on fixing the mistakes of predecessors [73,241]. Extreme gradient boosting (XGBoost) is also a powerful gradient boosting tree algorithm for urban FSM and is capable of integrating structured data [61,105,177]. This approach is suitable for solving classification problems and analyzing complex interactions among various flood causative factors [177]. Gradient boosting is also an effective tool for urban FSM [97] and it builds a simple decision tree model for

initial predictions and calculates the residuals of the prediction [242]. For every prediction, it builds a new decision tree while improving the accuracy of the previous model and the final model is the combination of all the predictions.

6. Discussion

6.1. Urban FSM vs. Non-Urban FSM

While FSM has been extensively studied across diverse landscapes, the unique challenges presented by urban environments necessitate a more nuanced approach compared to non-urban areas. Urban landscapes are characterized by impervious surfaces, dense infrastructure—such as roads and buildings—and dynamic anthropogenic factors, all of which exacerbate surface runoff and reduce drainage capacity during heavy rainfall events. These factors, combined with rapid urbanization, population growth, and the urban heat island effect, significantly contribute to the heightened flood risk in these regions.

In the context of the Anthropocene, where human activities increasingly shape the planet's environmental processes, urban areas reflect a convergence of natural and anthropogenic influences. The complexity of flood susceptibility in these regions is further heightened by alteration of natural hydrological cycles, with human interventions such as altered drainage systems, land reclamation, and intensive infrastructure development complicating flood prediction and mitigation. The anthropogenic footprint in urban environments demands that FSM approaches account not only for natural factors but also the dynamic and ever-evolving urban landscapes and infrastructures. In contrast, non-urban areas are typically governed by more predictable and stable hydrological processes. These regions often retain natural landscapes, and flood-prone routes are relatively consistent, making FSM in non-urban environments less complex and more stable for analysis.

Thus, urban FSM is of paramount importance in the Anthropocene due to an increased contribution of human-induced factors, necessitating the consideration of various scenarios that reflect both the natural environment and the built infrastructure. In comparison, non-urban FSM tends to rely on more traditional, stable modeling approaches that focus primarily on natural hydrological variables. Given these inherent complexities, urban FSM is more critical in informing flood resilience strategies, demanding a tailored approach that accounts for the multifaceted urban dynamics influencing flood susceptibility.

6.2. Remote Sensing (RS) Data Resolution and Suitability

In context of data availability for urban FSM, researchers have often faced challenges in obtaining data with appropriate granularity and quality from various repositories. However, recent advancements in satellite data have provided a promising solutions [243]. Improvements in the resolution, accuracy, and availability of satellite data have enabled the development of more robust modeling approaches [244]. This progress allows for improved calibration and validation through the integration of remote sensing derived flood extents and hydrological parameters. As a result, ongoing research continues to leverage remote sensing to advance flood susceptibility mapping, with a particular focus on optimizing data processing and model integration.

Satellite-based remote sensing data have significantly advanced urban FSM by providing high spatial and temporal resolution datasets such as LIDAR, Sentinel, Landsat, and SRTM [124,125]. However, the integration of RS data faces certain challenges, which must be carefully addressed for effective urban FSM in different regions worldwide. Studies often utilize 30-meter resolution SRTM DEMs and GLOBE DEMs to balance granularity and spatial coverage [80]; however, this may be insufficient for highly urbanized, dense vegetation and flat terrain areas. Sometimes, minor inaccuracies in elevation data may results in significant errors in urban FSM [125]. High-resolution DEMs such as LIDAR, SAR,

and Sentinel offer increased precision with an in-depth and detailed overview of spatial coverage but face constraints related to availability, cost, and computational demand [124]. Therefore, the selection of DEMs often depends on the extent of the study area, precision criteria, and suitability of computational expertise.

For data-scarce regions, studies have integrated satellite-derived remote sensing rainfall data for urban FSMs. However, this may contain biases and correction is needed to improve accuracy in urban FSM. To solve this issue, remote sensing data such as CHIRPS rainfall data can be incorporated with ground-based observational data and social media data in urban FSM [61]. Differences in spatial and temporal resolutions among datasets may create inconsistencies in urban FSM analysis. For example, fine-resolution topographic data may not align with coarse-resolution precipitation/land use land cover data. Therefore, integrating topographic, precipitation, and other flood-influencing datasets at comparable spatial and temporal scales is essential in urban FSM analysis. For land use land cover datasets, MODIS data with a resolution of 500 m are suitable for broad regional assessments [81]; however, they lack detailed coverage of the urban environment, whereas Sentinel-2 data with a resolution of 2 m offer greater granularity and details of smaller features [23]. For some regions, these high-resolution datasets present challenges in terms of computational demand, storage constraints, and potentially high costs. Therefore, some studies gather more information about the landscape of the study area and utilize Landsat 8, TM/ETM, and OLI data to calculate the normalized difference vegetation index (NDVI) and normalized difference built-up index (NDBI) to evaluate vegetation coverage and spread of impervious surface areas for urban FSM [105,107,109].

Environmental pollutants, such as aerosols, particulate matter, and smog, can significantly impact the quality of remote sensing data, often leading to inaccuracies in reflectance values. These pollutants can also alter the spectral signatures of surface features, making it difficult to differentiate between various land cover types. Optical sensors face additional challenges from clouds, particularly thick or persistent ones, which can obstruct data collection over large areas, especially in regions with frequent or seasonal cloud cover. To address these issues and enhance the accuracy, reliability, and usability of remote sensing data, several post-processing techniques are applied. Atmospheric distortions caused by pollutants can be corrected using methods like dark object subtraction. Georeferencing ensures satellite images are aligned with a standardized coordinate system, facilitating accurate mapping. Furthermore, techniques such as majority filtering and spatial smoothing are employed to minimize minor classification errors and create a more uniform spatial distribution of classified pixels.

6.3. Frequently Used Parameters by Region and Contribution to Urban FSM

Various sets of parameters and approaches have been used to map urban flood susceptibility in the literature. The wide-ranging set of parameters in susceptibility mapping offers researchers a robust perspective for evaluating the level of urban flood susceptibility. Understanding the strength and effectiveness of parameters is also important for researchers for more accurate susceptibility analysis. Research on urban flood susceptibility generally involves the use of 10-15 different parameters, such as slope, elevation, land use land cover, rainfall, distance from roads, distance from rivers, topographic wetness index (TWI), soil, geology, etc. The selection of parameters typically depends on the topography, hydrology, and climatic and meteorological characteristics of the study area and the suitability of available datasets. The most frequently used parameters in urban FSM are listed in Figure 6. While some researchers have noted that rainfall, soil, and land use land cover are the most useful parameters for urban FSM [157], some researchers have shown that land use land cover and altitude are the most effective parameters [80].

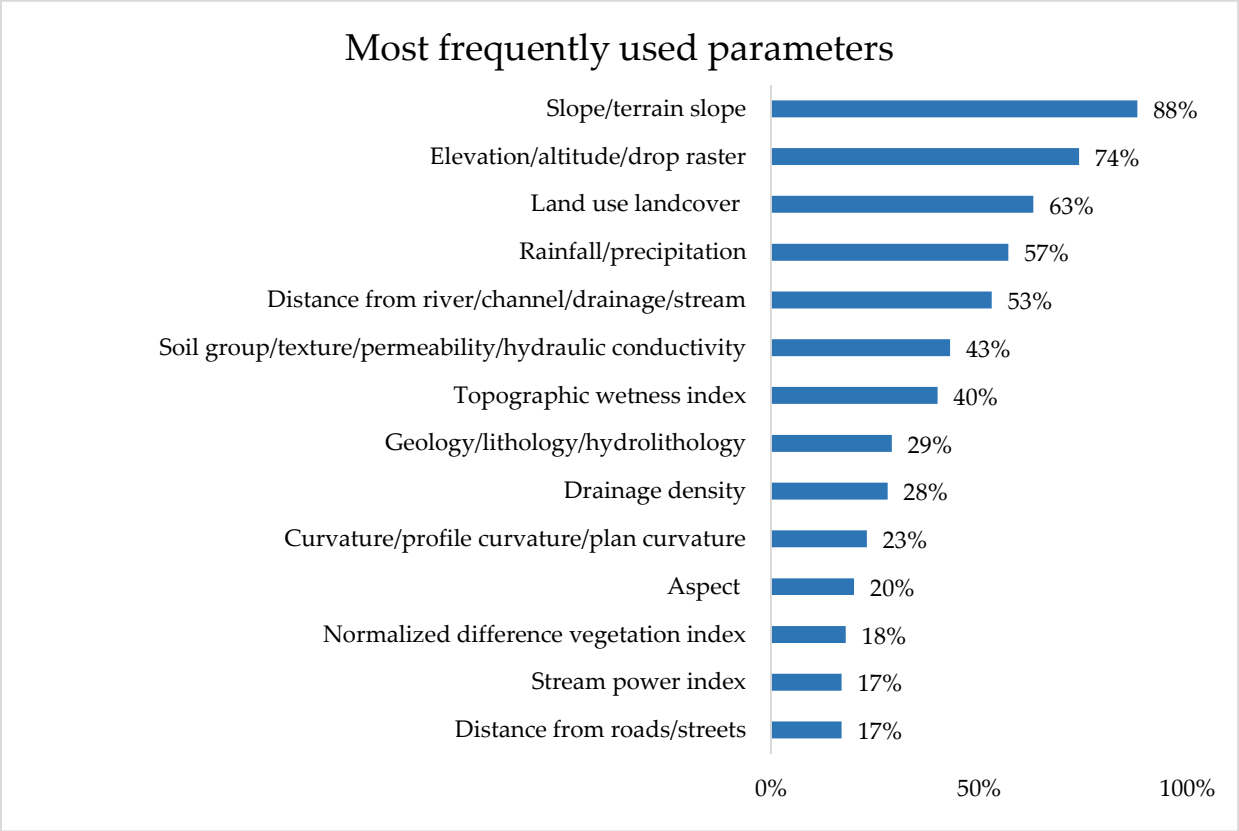

Figure 6. Frequently used urban FSM parameters in the literature.

If urban regions are located closer to mountainous areas or contain elevation differences, elevation, relative elevation, or slope gradient can be very effective parameters for urban FSM in those regions [145]. Tianhe and Panyu are two different districts of Guangdong Province, China. Tianhe city has high elevation in the northern part and low elevation in the southern part. Owing to this high elevation difference, elevation plays a crucial role in urban FSM in this area. Thus, in [104], researchers utilized slope, relative elevation, and standard deviation of elevation with other flood-conditioning factors in urban flood susceptibility analysis in this area. In contrast, slope is not the most effective parameter for urban FSM in flat regions [245]. If an urban region contains major water bodies, drainage density/distance to river can be a very effective parameter for urban FSM [60,73,116]. Therefore, the "distance from river/water bodies" or "drainage/channel/river density" is considered an important parameter in mapping urban flood susceptibility in these regions.

Rainfall is one of the most prominent drivers of urban flooding and its intensity, duration, frequency, and spatial distribution play important roles in urban FSM in various geographic regions [246]. Urban FSM in high-latitude regions should consider seasonal rainfall and its interaction with snowfall and melting patterns [247,248]. On the other hand, urban FSM in mountainous regions should account for spatial rainfall variability and rainfall intensity [145,249]. In addition, urban FSM in coastal regions must account for the frequency of intense rainfall alongside the tide level and rainfall intensity [250,251]. The effectiveness of land use land cover in urban FSMs is universally important, as it provides essential information for identifying critical areas for intervention [252]. However, it needs to be supplemented with region-specific factors such as soil type, drainage density, and geology to ensure robust urban FSM analysis [253].

Researchers have used more than 30 parameters in urban FSM analysis in different regions. Among the studies we have included in our review, 88% of them incorporate slope in urban FSM analysis, followed by elevation (74%), land use land cover (63%), rainfall

(57%), distance from water body (53%), soil properties (43%), TWI (40%), geology (29%), drainage density (28%), curvature (23%), aspect (20%), normalized difference vegetation index (18%), stream power index (17%), and distance from roads (17%). This preference rate also aligns with other studies [2]. The frequency and significance of these indicators stems from its direct and indirect influence on the hydrological, geological, and anthropogenic factors governing urban flood dynamics.

6.4. Urban FSM Model Performances

The approaches researchers have used for urban FSM are very different from one another on the basis of their expert opinions and ease of application. These approaches have their own strengths and weaknesses and can produce various uncertainties in urban FSM. Therefore, the approaches selected for urban FSM represent the spatially continuous and cumulative nature of the influence of parameters on the flood susceptibility mechanism. In addition, the selection of an appropriate methodology also depends on the spatial scale and availability of large/historical datasets, computational resources, and specific objective and accuracy requirements. For example, to implement machine learning models such as support vector machines, random forests, and artificial neural networks, large datasets are needed to train the models [153,199,254]. The most frequently used methods and their advantages and limitations in urban FSM are listed in Table 2. Although no single method is universally superior for urban FSM, combining different approaches can significantly enhance the accuracy and reliability of flood susceptibility assessments.

Researchers have utilized 2–3 different machine learning models to map urban flood susceptibility and compare and validate the results for better accuracy [61,73,103,104,255]. These integrative approaches help improve the precision of urban FSM and support the development of more robust and effective urban flood management and mitigation strategies [256,257]. Urban flooding is the outcome of multiple factors, including changes in land use land cover, deforestation, overwhelming drainage capacity, and climate change effects [258]. Therefore, the associations between flood occurrence and flood-conditioning factors are complex and nonlinear [259]. Researchers have reported that flood events usually have a nonlinear structure because of their complex mechanism [2,142,199,260,261]. These nonlinear flood characteristics have prompted researchers to move from traditional methods to advanced soft computing methods which offer higher accuracy in urban FSM [2]. When the predictors and target variables are nonlinear and complex, ML models surpass statistical models in terms of accuracy [73].

Researchers have compared various model performances in urban FSM and highlighted that decision tree based machine learning (ML) models perform better compared to frequency ratio models, where the random forest model is considered one of the best ML models, with an accuracy of 85% [73]. This finding is also consistent with various natural hazard susceptibility analyses [262–264]. Studies have utilized support vector machines and highlighted their robustness in handling nonlinear data, which reflects a consistent accuracy of approximately 85% to 87% depending on the urban landscape [142,181]. In [103], the authors incorporated both a support vector machine (SVM) and convolutional neural network (CNN) and reported that the CNN performed slightly better than the SVM model. The authors of [105] also highlighted that random forest and extreme gradient boosting (XGBoost) demonstrate better performance in urban FSM, achieving a model accuracy greater than 80%. Some studies have used artificial neural networks (ANNs) and highlighted that ANNs are very sensitive to noise and may overestimate highly flood-susceptible areas [105]. In [18], the authors utilized logistic regression (LR), frequency ratio (FR), Shannon's entropy (SE), and certainty factor (CF) to map urban flood susceptibility, and the LR performed better than the other models and the prediction rate was 75.4%. The authors of [169] also

reported similar results, and the LR prediction rate was 76%. Studies frequently use the analytical hierarchy process (AHP), which is based on individual judgment and expert opinions, to rank the parameters [23]. As there is a great chance of developing unreliability while applying the AHP, researchers utilize a consistency ratio (CR) to validate the ranking and the CR is considered acceptable if it is less than 0.1 [23,60]. In [79], the authors utilized evidential belief function (EBF) and fuzzy gamma operator (FGO). FGO performed better than EBF and the model accuracies were 71% and 69%, respectively.

In urban FSM, there is a qualitative difference between traditional and deep learning training samples [265,266]. Traditional methods such as analytical hierarchy process (AHP) and logistic regression depend on low-dimensional and structured datasets [117], whereas deep learning models require multidimensional and large datasets, which allows them to capture more complex interactions [83,267]. Deep learning models are capable of detecting nonlinear relationships and accommodating greater variability in flood causative parameters while training the datasets [220,268]. This helps to capture fine-grained spatial patterns and temporal dynamics in urban flood susceptibility. Owing to their ability to leverage and learn high-dimensional and complex datasets, deep learning models have shown higher accuracy in urban FSM particularly in densely populated urban areas [142,269]. On the other hand, traditional methods are effective in handling small and structured data; however, they often struggle to capture flood dynamics in complex urban landscapes and where flood causative parameters are interconnected. Therefore, traditional approaches pose quality challenges related to the training samples used in urban flood mapping approaches [171].

Table 2. Frequently used methods to map urban flood susceptibility and their advantages and limitations.

No.	Methods	Advantages	Limitations	Accuracy Remarks
1	Analytical hierarchy process	Simple and cost-effective approach. It does not require complex mathematical models and sophisticated computational resource [118]. Allows for the assignment of various weights on flood causative factors based on their importance [60].	Time-consuming for large datasets. Sensitive to weight changes. Limited control in real-time data. High subjectivity as it relies on expert opinions.	Model accuracy based on AUC is 84–87.3% [84,88]
2	Support vector machine	Useful in working complex and nonlinear datasets [109]. Can handle both binary (flooded vs. non-flooded) and multi-class classification.	Requires historical/large flood datasets to train the model.	Model accuracy based on AUC is 82–96.2% [105,199,270]
3	Artificial neural network	Very effective in capturing complex and nonlinear datasets [191].	Computationally intensive and prone to overfitting with limited data.	Model accuracy based on AUC is 83% [105]
4	Random forest	Can handle missing data without significant loss in performance, which is useful in urban flood mapping [105].	In areas with minimal historical flood records, RF might not perform effectively.	Model accuracy based on AUC is 85–96% [73,105,112]
5	Weighted overlay	Simple and easy to implement. Weights can be adjusted based on expert opinion, local knowledge, and empirical data, making it feasible to adjust the model to specific urban conditions [23]. This approach is effective for analyzing large areas because it can combine multiple layers of spatial data into one output layer [126].	Weights remain constant for entire study area. Use can be challenging in urban environments where the influence of flood causative factors may vary in different locations. Mostly relies on expert opinions.	Model accuracy based on AUC is 87.5% [80]

Table 2. *Cont.*

No.	Methods	Advantages	Limitations	Accuracy Remarks
6	Logistic regression	Compared to complex ML models, logistic regression can work effectively on smaller dataset [110]. Urban flood mapping often deals with two classes (flood-prone areas and non-flood-prone areas); LR is suitable for these classification problems.	If the dataset is too small, it can overfit the model. Model assumes linear relationship with variables.	Model accuracy based on AUC is 92–93% [199,270]
7	Frequency ratio	Can be less effective when working with high-dimensional data with many flood causative factors [18].	FR is not a good fit if historical flood data are unavailable.	Model accuracy based on AUC is 72–89.5% [73,270]
8	Extreme gradient boosting	Popular due to high prediction accuracy [105]. Can handle large numbers of datasets without significant degradation in performance. Less sensitive to missing data.	Risk of overfitting training data.	Model accuracy based on AUC is 84–87% [73,105]
9	Multi-criteria decision analysis	Provides a structured framework for integration of multiple flood causative factors.	Mostly relies on expert opinions, which can create a bias [116].	Model accuracy is 92% [271]
10	Convolutional neural network	Can handle complex (spatial, temporal, and textual) datasets, making it suitable for urban FSM [103]. Automatically learns hierarchical features from the input data, which makes it useful for urban FSM.	Model performance heavily depends on quality of input data [104].	Model accuracy based on AUC is 87% [112]
11	Fuzzy technique	Can be easily integrated with GISs, allowing for spatial representation and detailed analysis of flood susceptibility [189]. Does not require large datasets for training.	Cannot capture spatial correlation between neighboring areas [87].	Model accuracy based on AUC is 91.6% [272]
12	Gradient boosting	Allows for fine-tuning hyperparameters to optimize performance for specific flood mapping tasks [107].	Can be very sensitive to noisy data [73].	Model accuracy based on AUC is 83% [73]

6.5. Urban FSM Model Validation

Accurately mapping urban flood-susceptible zones and model validation are crucial tasks in urban FSM. In one study, researchers utilized a range of validation approaches to evaluate the performance of machine learning (ML) and other models in urban FSM. The researchers employed multiple DT-based ML models, namely, DT, adaptive boosting (AdaBoost), gradient boosting (GdBoost), extreme gradient boosting (XGBoost), and random forest (RF) models for urban FSM, as well as various validation techniques, including the confusion matrix, K-fold cross validation, overall accuracy, precision recall, AUC curve, and F-1 score, to select the best-performing decision tree-based machine learning models [73]. The AUC value is highest for the RF model (0.85), followed by AdaBoost (0.74), GdBoost (0.83), and XGBoost (0.84). The researchers utilized the K-fold cross validation method to validate training samples, and this method is useful, particularly when the sample size is small [273]. K-fold cross validation revealed that RF achieved the highest mean score of 0.80, followed by XGBoost (0.77), GdBoost (0.75), and AdaBoost (0.73) [73].

Another study utilized random forest, naïve Bayes, and extreme gradient boosting for urban FSM and employed the kappa index, mean absolute error, RMSE (root mean square error), and Pearson's correlation coefficients to validate the efficiency of machine learning

model performances in urban FSM [274]. Among them, the highest-performing model was random forest (84.7%), followed by the XGB model (83.1%) and the naïve Bayes model (82.1%). Another study validated urban FSM generated by the AHP (analytical hierarchy process) approach using the AUC (area under the curve) and achieved AUC values of 0.84 or 84%, which represent very good accuracy [84]. This finding also aligns with other urban FSM studies too [275,276]. Another urban FSM study which employed AHP reported AUC values greater than 0.90, which represents excellent accuracy [277]. Different studies have employed sets of various validation approaches to evaluate model performances; however, no single validation method is universally superior. While diverse validation metrics provide valuable insights into model performance, their application should be tailored to the specific dataset and context. Employing multiple validation methods enhances confidence in the results and ensures robust decision-making in urban FSM.

6.6. Urban FSM Challenges

There are several limitations in the current state of urban FSM, particularly in regions where data availability is limited.

Scarcity of hydrological/meteorological data: Data scarcity and complex urban mechanisms are two major obstacles in urban FSM [145]. Sometimes, the lack of data on hydro-meteorological and hydraulic characteristics makes it challenging to understand urban flood mechanisms. In some regions, historical flood data, up-to-date meteorological data, and drainage system data are not easily accessible, which hinders the development of reliable flood susceptibility models in these regions.

Availability of high-resolution RS data: One notable challenge is the lack of available high spatial and temporal resolution data, which is crucial for more accurate urban FSM. For example, it is difficult to obtain very high-resolution spatiotemporal rainfall data and detailed sewer drainage lines in developing nations. Integrating data from multiple sensors and using global datasets may solve this issue.

Integration of diverse datasets: Another challenge lies in integrating diverse data sources, such as ground survey data, social media data in urban FSM analysis. These data sources vary in scale, format, and quality and pose challenges in combining them in urban FSMs. While social media and real-time data have emerged as valuable resources for urban flood mapping, their integration into current urban FSM remains underutilized. Standardizing the data formats and projections while performing data preprocessing can reduce this problem in urban FSM analysis. The incorporation of these data sources could significantly increase the precision and accuracy of urban flood susceptibility assessments by providing timely and localized information that traditional data sources may not capture. The development of standardized approaches for integrating these heterogeneous data sources will ensure more reliable and comprehensive urban flood susceptibility assessments. Future research should focus on effectively integrating these dynamic data sources to improve urban flood mapping approaches.

Model accuracy: Urban FSM analysis output may introduce accuracy issues due to the complexity of urban landscapes, diverse data sources, and varying model assumptions. Integrating multiple models and comparing model performances will help identify the discrepancies and increase the accuracy.

7. Conclusions

Urban FSM is an effective risk reduction strategy for hazard management, particularly as urbanization and climate change intensify flood risks globally. This paper provides an in-depth overview of urban FSM approaches, focusing on the effectiveness, strengths, and limitations of traditional, data-driven, and advanced big data approaches. It explores the

suitability of remote sensing datasets and flood causative parameters and their relationships with flood events in various regions. Our comprehensive analysis revealed three major challenges in urban FSM implementation: (1) the complexity of built-up environments that create unique flood dynamics, (2) the limited availability of high-resolution data in many urban areas, and (3) the need for better integration of multiple data sources to capture diverse flooding mechanisms. Additionally, our study also serves as a resource for researchers, urban planners, and policymakers, helping them better understand urban flood susceptibility mapping and enhance resilience through informed decision-making.

The novelty of this work lies in its emphasis on selecting flood susceptibility parameters based on the landscape and hydrological characteristics of each study area, as well as the fusion of cutting-edge multidisciplinary approaches to enhance mapping accuracy and precision. It provides a comprehensive overview regarding the suitability of remote sensing datasets for urban FSM in varying geographic and topographic characteristics in urban contexts. This work provides valuable insights for improving future urban FSM research, such as (1) developing standardized protocols for urban flood parameter selection based on local contexts, (2) establishing open access platforms for high-resolution urban data sharing, and (3) creating frameworks for integrating multiple data sources and modeling approaches. These steps will enable urban planners and policymakers to better implement FSM for enhanced flood resilience across diverse urban settings.

Future research should explore holistic approaches that integrate both local and regional flood causative factors to increase the accuracy and reliability of urban FSM. The combination of machine learning techniques with hydrological models also offers significant potential, particularly in scenarios with limited data availability. The incorporation of flood data from local communities, such as geotagged photos and real-time flood reports, can aid official flood mapping and improve the precision and accuracy of future flood susceptibility mapping. Moreover, future research should also incorporate various climate change and land use land cover projection scenarios into urban FSM for resilient urban planning strategies and mitigating potential losses.

Author Contributions: Conceptualization, T.I. and A.M.M.; methodology, T.I.; formal analysis, T.I., E.B.Z., M.A., and A.M.M.; writing—original draft preparation, T.I.; writing—review and editing, T.I., E.B.Z., M.A., and A.M.M.; visualization, T.I.; supervision, A.M.M. All authors have read and agreed to the published version of the manuscript.

Funding: This research received no external funding.

Data Availability Statement: No data was generated in this paper. The original data presented in the study are openly available in web of science.

Conflicts of Interest: The authors declare no conflicts of interest.

References

1. Jonkman, S.N. Global perspectives on loss of human life caused by floods. *Nat. Hazards* **2005**, *34*, 151–175. [CrossRef]
2. Kaya, C.M.; Derin, L. Parameters and methods used in flood susceptibility mapping: A review. *J. Water Clim. Change* **2023**, *14*, 1935–1960. [CrossRef]
3. Dharmarathne, G.; Waduge, A.; Bogahawaththa, M.; Rathnayake, U.; Meddage, D. Adapting cities to the surge: A comprehensive review of climate-induced urban flooding. *Results Eng.* **2024**, *22*, 102123. [CrossRef]
4. Ma, B.; Wu, Z.; Hu, C.; Wang, H.; Xu, H.; Yan, D. Process-oriented SWMM real-time correction and urban flood dynamic simulation. *J. Hydrol.* **2022**, *605*, 127269. [CrossRef]
5. Rodriguez, E.; Berrocal, F.; Rodriguez, A. Flood hazards in Extremadura and associated impacts. *Investig. Geogr.* **2021**, *75*, 121–137.
6. Tellman, B.; Sullivan, J.A.; Kuhn, C.; Kettner, A.J.; Doyle, C.S.; Brakenridge, G.R.; Erickson, T.A.; Slayback, D.A. Satellite imaging reveals increased proportion of population exposed to floods. *Nature* **2021**, *596*, 80–86. [CrossRef]
7. Dewan, T.H. Societal impacts and vulnerability to floods in Bangladesh and Nepal. *Weather Clim. Extrem.* **2015**, *7*, 36–42. [CrossRef]

8. Collins, T. *Two Billion People Vulnerable to Floods by 2050; Number Expected to Double or More in Two Generations Due to Climate Change, Deforestation, Rising Seas, Population Growth Retrieved October 30, 2006*; United Nations University: Tokyo, Japan, 2004.
9. Tang, X.; Tian, J.; Huang, X.; Shu, Y.; Liu, Z.; Long, S.; Xue, W.; Liu, L.; Lin, X.; Liu, W. A novel machine learning-based framework to extract the urban flood susceptible regions. *Int. J. Appl. Earth Obs. Geoinf.* **2024**, *132*, 104050. [CrossRef]
10. Yariyan, P.; Avand, M.; Abbaspour, R.A.; Torabi Haghighi, A.; Costache, R.; Ghorbanzadeh, O.; Janizadeh, S.; Blaschke, T. Flood susceptibility mapping using an improved analytic network process with statistical models. *Geomat. Nat. Hazards Risk* **2020**, *11*, 2282–2314. [CrossRef]
11. Majid, S.I.; Kumar, M.; Sahu, N.; Kumar, P.; Tripathi, D.K. Application of ensemble fuzzy weights of evidence-support vector machine (Fuzzy WofE-SVM) for urban flood modeling and coupled risk (CR) index for ward prioritization in NCT Delhi, India. *Environ. Dev. Sustain.* **2024**, 1–39. [CrossRef]
12. Du, S.; Cheng, X.; Huang, Q.; Chen, R.; Ward, P.J.; Aerts, J.C. Brief communication: Rethinking the 1998 China floods to prepare for a nonstationary future. *Nat. Hazards Earth Syst. Sci.* **2019**, *19*, 715–719. [CrossRef]
13. Masoumi, Z. Flood susceptibility assessment for ungauged sites in urban areas using spatial modeling. *J. Flood Risk Manag.* **2022**, *15*, e12767. [CrossRef]
14. Boller, D.; Moy de Vitry, M.; Wegner, J.D.; Leitão, J.P. Automated localization of urban drainage infrastructure from public-access street-level images. *Urban Water J.* **2019**, *16*, 480–493. [CrossRef]
15. Zhang, W.; Villarini, G.; Vecchi, G.A.; Smith, J.A. Urbanization exacerbated the rainfall and flooding caused by hurricane Harvey in Houston. *Nature* **2018**, *563*, 384–388. [CrossRef]
16. Mahmoud, S.H.; Gan, T.Y. Urbanization and climate change implications in flood risk management: Developing an efficient decision support system for flood susceptibility mapping. *Sci. Total Environ.* **2018**, *636*, 152–167. [CrossRef]
17. Daksiya, V.; Mandapaka, P.V.; Lo, E.Y. Effect of climate change and urbanisation on flood protection decision-making. *J. Flood Risk Manag.* **2021**, *14*, e12681. [CrossRef]
18. Gupta, L.; Dixit, J. Assessment of urban flood susceptibility and role of urban green space (UGS) on flooding susceptibility using GIS-based probabilistic models. *Environ. Monit. Assess.* **2023**, *195*, 1518. [CrossRef]
19. Traoré, K.; Fowe, T.; Ouédraogo, M.; Zorom, M.; Bologo/Traoré, M.; Toé, P.; Karambiri, H. Mapping urban flood susceptibility in Ouagadougou, Burkina Faso. *Environ. Earth Sci.* **2024**, *83*, 561. [CrossRef]
20. Wu, Z.; Shen, Y.; Wang, H.; Wu, M. Assessing urban flood disaster risk using Bayesian network model and GIS applications. *Geomat. Nat. Hazards Risk* **2019**, *10*, 2163–2184. [CrossRef]
21. Kumar, M.; Singh, R.; Singh, A.; Pravesh, R.; Majid, S.I.; Tiwari, A. Case study 6: Urban flood susceptibility modelling of Srinagar using novel fuzzy multi-layer perceptron neural network. In *Geographic Information Systems in Urban Planning and Management*; Springer: Singapore, 2023; pp. 221–238.
22. Rentschler, J.; Avner, P.; Marconcini, M.; Su, R.; Strano, E.; Vousdoukas, M.; Hallegatte, S. Global evidence of rapid urban growth in flood zones since 1985. *Nature* **2023**, *622*, 87–92. [CrossRef]
23. Hirwa, H.; Ngwijabagabo, H.; Minani, M.; Tuyishime, S.P.C.; Habimana, I. Geospatial Assessment of Urban Flood Susceptibility Using AHP-Based Multi-Criteria Technique: Case Study of Musanze, Rwanda. *Rwanda J. Eng. Sci. Technol. Environ.* **2023**, *5*, 24. [CrossRef]
24. Tayyab, M.; Zhang, J.; Hussain, M.; Ullah, S.; Liu, X.; Khan, S.N.; Baig, M.A.; Hassan, W.; Al-Shaibah, B. Gis-based urban flood resilience assessment using urban flood resilience model: A case study of peshawar city, khyber pakhtunkhwa, pakistan. *Remote Sens.* **2021**, *13*, 1864. [CrossRef]
25. Zheng, Z.; Gao, J.; Ma, Z.; Wang, Z.; Yang, X.; Luo, X.; Jacquet, T.; Fu, G. Urban flooding in China: Main causes and policy recommendations. *Hydrol. Process.* **2016**, *30*, 1149–1152. [CrossRef]
26. Sui, X.; Yang, Z.-L.; Shepherd, M.; Niyogi, D. Global scale assessment of urban precipitation anomalies. *Proc. Natl. Acad. Sci. USA* **2024**, *121*, e2311496121. [CrossRef]
27. Dano, U.L.; Balogun, A.-L.; Matori, A.-N.; Wan Yusouf, K.; Abubakar, I.R.; Said Mohamed, M.A.; Aina, Y.A.; Pradhan, B. Flood susceptibility mapping using GIS-based analytic network process: A case study of Perlis, Malaysia. *Water* **2019**, *11*, 615. [CrossRef]
28. Youssef, A.M.; Pradhan, B.; Sefry, S.A. Flash flood susceptibility assessment in Jeddah city (Kingdom of Saudi Arabia) using bivariate and multivariate statistical models. *Environ. Earth Sci.* **2016**, *75*, 12. [CrossRef]
29. de Melo, S.K.; Almeida, A.K.; de Almeida, I.K. Multicriteria analysis for flood risk map development: A hierarchical method applied to Brazilian cities. *Environ. Sci. Pollut. Res.* **2023**, *30*, 80311–80334. [CrossRef]
30. dos Santos, J.C.; Lyra, G.B.; Abreu, M.C.; Andrade, C.D.; Moster, C.; Cunha-Zeri, G.; Zeri, M. Flood-prone areas based on physiographic indices and multi-criteria assessment for the basins of Ubatuba, on the mountainous North Coast of São Paulo State, Brazil. *Environ. Earth Sci.* **2023**, *82*, 517. [CrossRef]
31. Ramkar, P.; Yadav, S.M. Flood risk index in data-scarce river basins using the AHP and GIS approach. *Nat. Hazards* **2021**, *109*, 1119–1140. [CrossRef]

32. Abdrabo, K.I.; Kantoush, S.A.; Esmaiel, A.; Saber, M.; Sumi, T.; Almamari, M.; Elboshy, B.; Ghoniem, S. An integrated indicator-based approach for constructing an urban flood vulnerability index as an urban decision-making tool using the PCA and AHP techniques: A case study of Alexandria, Egypt. *Urban Clim.* **2023**, *48*, 101426. [CrossRef]
33. Miranda, F.; Franco, A.B.; Rezende, O.; da Costa, B.B.; Najjar, M.; Haddad, A.N.; Miguez, M. A GIS-Based Index of Physical Susceptibility to Flooding as a Tool for Flood Risk Management. *Land* **2023**, *12*, 1408. [CrossRef]
34. Shokouhifar, Y.; Lotfirad, M.; Esmaeili-Gisavandani, H.; Adib, A. Evaluation of climate change effects on flood frequency in arid and semi-arid basins. *Water Supply* **2022**, *22*, 6740–6755. [CrossRef]
35. Li, C.; Sun, N.; Lu, Y.; Guo, B.; Wang, Y.; Sun, X.; Yao, Y. Review on urban flood risk assessment. *Sustainability* **2022**, *15*, 765. [CrossRef]
36. Caprario, J.; Rech, A.S.; Tasca, F.A.; Finotti, A.R. Influence of drainage network and compensatory techniques on urban flooding susceptibility. *Water Sci. Technol.* **2019**, *79*, 1152–1163. [CrossRef]
37. Vojtek, M.; Vojteková, J. Flood susceptibility mapping on a national scale in Slovakia using the analytical hierarchy process. *Water* **2019**, *11*, 364. [CrossRef]
38. Santangelo, N.; Santo, A.; Di Crescenzo, G.; Foscari, G.; Liuzza, V.; Sciarrotta, S.; Scorpio, V. Flood susceptibility assessment in a highly urbanized alluvial fan: The case study of Sala Consilina (southern Italy). *Nat. Hazards Earth Syst. Sci.* **2011**, *11*, 2765–2780. [CrossRef]
39. Tariq, A.; Yan, J.; Ghaffar, B.; Qin, S.; Mousa, B.; Sharifi, A.; Huq, M.E.; Aslam, M. Flash flood susceptibility assessment and zonation by integrating analytic hierarchy process and frequency ratio model with diverse spatial data. *Water* **2022**, *14*, 3069. [CrossRef]
40. Al-Abadi, A.M.; Shahid, S.; Al-Ali, A.K. A GIS-based integration of catastrophe theory and analytical hierarchy process for mapping flood susceptibility: A case study of Teeb area, Southern Iraq. *Environ. Earth Sci.* **2016**, *75*, 687. [CrossRef]
41. Kuriqi, A.; Hysa, A. Multidimensional aspects of floods: Nature-based mitigation measures from basin to river reach scale. In *Nature-Based Solutions for Flood Mitigation: Environmental and Socio-Economic Aspects*; Springer: Cham, Switzerland, 2021; pp. 11–33.
42. Bibi, T.S.; Kara, K.G. Evaluation of climate change, urbanization, and low-impact development practices on urban flooding. *Heliyon* **2023**, *9*, e12955. [CrossRef]
43. Burgan, H.I.; Icaga, Y. Flood analysis using adaptive hydraulics (AdH) model in Akarcay Basin. *Tek. Dergi* **2019**, *30*, 9029–9051. [CrossRef]
44. Agonafir, C.; Lakhankar, T.; Khanbilvardi, R.; Krakauer, N.; Radell, D.; Devineni, N. A review of recent advances in urban flood research. *Water Secur.* **2023**, *19*, 100141. [CrossRef]
45. Termeh, S.V.R.; Kornejady, A.; Pourghasemi, H.R.; Keesstra, S. Flood susceptibility mapping using novel ensembles of adaptive neuro fuzzy inference system and metaheuristic algorithms. *Sci. Total Environ.* **2018**, *615*, 438–451. [CrossRef] [PubMed]
46. Wang, Y.; Hong, H.; Chen, W.; Li, S.; Pamučar, D.; Gigović, L.; Drobnjak, S.; Tien Bui, D.; Duan, H. A hybrid GIS multi-criteria decision-making method for flood susceptibility mapping at Shangyou, China. *Remote Sens.* **2018**, *11*, 62. [CrossRef]
47. Khoshkonesh, A.; Nazari, R.; Nikoo, M.R.; Karimi, M. Enhancing flood risk assessment in urban areas by integrating hydrodynamic models and machine learning techniques. *Sci. Total Environ.* **2024**, *952*, 175859. [CrossRef]
48. Duan, L.; Liu, C.; Xu, H.; Pan, H.; Liu, H.; Yan, X.; Liu, T.; Yang, Z.; Liu, G.; Dai, X. Susceptibility assessment of flash floods: A bibliometrics analysis and review. *Remote Sens.* **2022**, *14*, 5432. [CrossRef]
49. Tang, Y.; Sun, Y.; Han, Z.; Wu, Q.; Tan, B.; Hu, C. Flood forecasting based on machine learning pattern recognition and dynamic migration of parameters. *J. Hydrol. Reg. Stud.* **2023**, *47*, 101406. [CrossRef]
50. Darabi, H.; Choubin, B.; Rahmati, O.; Haghighi, A.T.; Pradhan, B.; Kløve, B. Urban flood risk mapping using the GARP and QUEST models: A comparative study of machine learning techniques. *J. Hydrol.* **2019**, *569*, 142–154. [CrossRef]
51. Shen, Y.; Morsy, M.M.; Huxley, C.; Tahvildari, N.; Goodall, J.L. Flood risk assessment and increased resilience for coastal urban watersheds under the combined impact of storm tide and heavy rainfall. *J. Hydrol.* **2019**, *579*, 124159. [CrossRef]
52. Karmakar, S.; Sherly, M.; Mohanty, M. Urban flood risk mapping: A state-of-the-art review on quantification, current practices, and future challenges. In *Advances in Urban Design and Engineering: Perspectives from India*; Springer: Singapore, 2022; pp. 125–156.
53. Rosenzweig, B.; Herreros Cantis, P.; Kim, Y.; Cohn, A.; Grove, K.; Brock, J.; Yesuf, J.; Mistry, P.; Welty, C.; McPhearson, T. The value of urban flood modeling. *Earth's Future* **2021**, *9*, e2020EF001739. [CrossRef]
54. Chen, Y.; Zhou, H.; Zhang, H.; Du, G.; Zhou, J. Urban flood risk warning under rapid urbanization. *Environ. Res.* **2015**, *139*, 3–10. [CrossRef]
55. Bekele, T.W.; Haile, A.T.; Trigg, M.A.; Walsh, C.L. Evaluating a new method of remote sensing for flood mapping in the urban and peri-urban areas: Applied to Addis Ababa and the Akaki catchment in Ethiopia. *Nat. Hazards Res.* **2022**, *2*, 97–110. [CrossRef]
56. Matyukira, C.; Mhangara, P. Advancement in the Application of Geospatial Technology in Archaeology and Cultural Heritage in South Africa: A Scientometric Review. *Remote Sens.* **2023**, *15*, 4781. [CrossRef]

57. Zhu, W.; Cao, Z.; Luo, P.; Tang, Z.; Zhang, Y.; Hu, M.; He, B. Urban Flood-Related Remote Sensing: Research Trends, Gaps and Opportunities. *Remote Sens.* **2022**, *14*, 5505. [CrossRef]
58. Xing, Z.; Yang, S.; Zan, X.; Dong, X.; Yao, Y.; Liu, Z.; Zhang, X. Flood vulnerability assessment of urban buildings based on integrating high-resolution remote sensing and street view images. *Sustain. Cities Soc.* **2023**, *92*, 104467. [CrossRef]
59. Jiménez-Jiménez, S.I.; Ojeda-Bustamante, W.; Ontiveros-Capurata, R.E.; Marcial-Pablo, M.d.J. Rapid urban flood damage assessment using high resolution remote sensing data and an object-based approach. *Geomat. Nat. Hazards Risk* **2020**, *11*, 906–927. [CrossRef]
60. de Moraes, R.B.F.; Gonçalves, F.V. Development, Application, and Validation of the Urban Flood Susceptibility Index. *Water Resour. Manag.* **2024**, *38*, 2511–2525. [CrossRef]
61. Zhu, X.; Guo, H.; Huang, J.J. Urban flood susceptibility mapping using remote sensing, social sensing and an ensemble machine learning model. *Sustain. Cities Soc.* **2024**, *108*, 105508. [CrossRef]
62. Islam, M.T.; Meng, Q. An exploratory study of Sentinel-1 SAR for rapid urban flood mapping on Google Earth Engine. *Int. J. Appl. Earth Obs. Geoinf.* **2022**, *113*, 103002.
63. Li, Y.; Martinis, S.; Wieland, M.; Schlaffer, S.; Natsuaki, R. Urban flood mapping using SAR intensity and interferometric coherence via Bayesian network fusion. *Remote Sens.* **2019**, *11*, 2231. [CrossRef]
64. Lammers, R.; Li, A.; Nag, S.; Ravindra, V. Prediction models for urban flood evolution for satellite remote sensing. *J. Hydrol.* **2021**, *603*, 127175. [CrossRef]
65. Munawar, H.S.; Hammad, A.W.; Waller, S.T. Remote sensing methods for flood prediction: A review. *Sensors* **2022**, *22*, 960. [CrossRef] [PubMed]
66. Sanyal, J.; Lu, X.X. Application of remote sensing in flood management with special reference to monsoon Asia: A review. *Nat. Hazards* **2004**, *33*, 283–301. [CrossRef]
67. Notti, D.; Giordan, D.; Caló, F.; Pepe, A.; Zucca, F.; Galve, J.P. Potential and limitations of open satellite data for flood mapping. *Remote Sens.* **2018**, *10*, 1673. [CrossRef]
68. Faisal Koko, A.; Yue, W.; Abdullahi Abubakar, G.; Hamed, R.; Noman Alabsi, A.A. Analyzing urban growth and land cover change scenario in Lagos, Nigeria using multi-temporal remote sensing data and GIS to mitigate flooding. *Geomat. Nat. Hazards Risk* **2021**, *12*, 631–652. [CrossRef]
69. Thanh Son, N.; Thi Thu Trang, N.; Bui, X.T.; Thi Da, C. Remote sensing and GIS for urbanization and flood risk assessment in Phnom Penh, Cambodia. *Geocarto Int.* **2022**, *37*, 6625–6642. [CrossRef]
70. Schumann, G.J.-P.; Neal, J.C.; Mason, D.C.; Bates, P.D. The accuracy of sequential aerial photography and SAR data for observing urban flood dynamics, a case study of the UK summer 2007 floods. *Remote Sens. Environ.* **2011**, *115*, 2536–2546. [CrossRef]
71. Mason, D.C.; Dance, S.L.; Cloke, H.L. Floodwater detection in urban areas using Sentinel-1 and WorldDEM data. *J. Appl. Remote Sens.* **2021**, *15*, 032003. [CrossRef]
72. Sy, H.M.; Luu, C.; Bui, Q.D.; Ha, H.; Nguyen, D.Q. Urban flood risk assessment using Sentinel-1 on the google earth engine: A case study in Thai Nguyen city, Vietnam. *Remote Sens. Appl. Soc. Environ.* **2023**, *31*, 100987.
73. Dey, H.; Shao, W.; Moradkhani, H.; Keim, B.D.; Peter, B.G. Urban flood susceptibility mapping using frequency ratio and multiple decision tree-based machine learning models. *Nat. Hazards* **2024**, *120*, 10365–10393. [CrossRef]
74. Michaelides, S.; Levizzani, V.; Anagnostou, E.; Bauer, P.; Kasparis, T.; Lane, J. Precipitation: Measurement, remote sensing, climatology and modeling. *Atmos. Res.* **2009**, *94*, 512–533. [CrossRef]
75. Funk, C.; Peterson, P.; Landsfeld, M.; Pedreros, D.; Verdin, J.; Shukla, S.; Husak, G.; Rowland, J.; Harrison, L.; Hoell, A. The climate hazards infrared precipitation with stations—A new environmental record for monitoring extremes. *Sci. Data* **2015**, *2*, 150066. [CrossRef] [PubMed]
76. Fletcher, R.; Fortin, M.-J. Introduction to spatial ecology and its relevance for conservation. In *Spatial Ecology and Conservation Modeling Applications with R*; Springer: Cham, Switzerland, 2018; pp. 1–13.
77. Casals-Carrasco, P.; Kubo, S.; Madhavan, B.B. Application of spectral mixture analysis for terrain evaluation studies. *Int. J. Remote Sens.* **2000**, *21*, 3039–3055. [CrossRef]
78. De Kok, R.; Schneider, T.; Ammer, U. Object based classification and applications in the Alpine forest environment. *Int. Arch. Photogramm. Remote Sens.* **1999**, *32*, 3–4.
79. Ramesh, V.; Iqbal, S.S. Urban flood susceptibility zonation mapping using evidential belief function, frequency ratio and fuzzy gamma operator models in GIS: A case study of Greater Mumbai, Maharashtra, India. *Geocarto Int.* **2022**, *37*, 581–606. [CrossRef]
80. Idrees, M.O.; Yusuf, A.; Mokhtar, E.S.; Yao, K. Urban flood susceptibility mapping in Ilorin, Nigeria, using GIS and multi-criteria decision analysis. *Model. Earth Syst. Environ.* **2022**, *8*, 5779–5791. [CrossRef]
81. Heidari, E.; Mahmoudzadeh, A.; Mansouri Daneshvar, M.R. Urban flood susceptibility evaluation and prediction during 2010–2030 in the southern watersheds of Mashhad city, Iran. *Environ. Syst. Res.* **2021**, *10*, 41. [CrossRef]
82. Pati, A.; Sahoo, B. Effect of low-impact development scenarios on pluvial flood susceptibility in a scantily gauged urban–peri-urban catchment. *J. Hydrol. Eng.* **2022**, *27*, 05021034. [CrossRef]

83. Ahmed, I.A.; Talukdar, S.; Shahfahad; Parvez, A.; Rihan, M.; Baig, M.R.I.; Rahman, A. Flood susceptibility modeling in the urban watershed of Guwahati using improved metaheuristic-based ensemble machine learning algorithms. *Geocarto Int.* **2022**, *37*, 12238–12266. [CrossRef]
84. Nsangou, D.; Kpoumié, A.; Mfonka, Z.; Ngouh, A.N.; Fossi, D.H.; Jourdan, C.; Mbele, H.Z.; Mouncherou, O.F.; Vandervaere, J.-P.; Ngoupayou, J.R.N. Urban flood susceptibility modelling using AHP and GIS approach: Case of the Mfoundi watershed at Yaoundé in the South-Cameroon plateau. *Sci. Afr.* **2022**, *15*, e01043. [CrossRef]
85. Nsangou, D.; Kpoumié, A.; Mfonka, Z.; Bateni, S.M.; Ngouh, A.N.; Ndam Ngoupayou, J.R. The mfoundi watershed at yaoundé in the humid tropical zone of Cameroon: A case study of urban flood susceptibility mapping. *Earth Syst. Environ.* **2022**, *6*, 99–120. [CrossRef]
86. Zeng, Z.; Lan, J.; Hamidi, A.R.; Zou, S. Integrating Internet media into urban flooding susceptibility assessment: A case study in China. *Cities* **2020**, *101*, 102697. [CrossRef]
87. Nourani, V.; Andaryani, S. Flood susceptibility mapping in densely populated urban areas using MCDM and fuzzy techniques. *IOP Conf. Ser. Earth Environ. Sci.* **2020**, *491*, 012003. [CrossRef]
88. Nguyen, H.N.; Fukuda, H.; Nguyen, M.N. Assessment of the Susceptibility of Urban Flooding Using GIS with an Analytical Hierarchy Process in Hanoi, Vietnam. *Sustainability* **2024**, *16*, 3934. [CrossRef]
89. Shafizadeh-Moghadam, H.; Valavi, R.; Shahabi, H.; Chapi, K.; Shirzadi, A. Novel forecasting approaches using combination of machine learning and statistical models for flood susceptibility mapping. *J. Environ. Manag.* **2018**, *217*, 1–11. [CrossRef] [PubMed]
90. Dahri, N.; Abida, H. Monte Carlo simulation-aided analytical hierarchy process (AHP) for flood susceptibility mapping in Gabes Basin (southeastern Tunisia). *Environ. Earth Sci.* **2017**, *76*, 302. [CrossRef]
91. Muthu, K.; Ramamoorthy, S. Evaluation of urban flood susceptibility through integrated Bivariate statistics and Geospatial technology. *Environ. Monit. Assess.* **2024**, *196*, 526. [CrossRef]
92. Debnath, J.; Debbarma, J.; Debnath, A.; Meraj, G.; Chand, K.; Singh, S.K.; Kanga, S.; Kumar, P.; Sahariah, D.; Saikia, A. Flood susceptibility assessment of the Agartala Urban Watershed, India, using machine learning algorithm. *Environ. Monit. Assess.* **2024**, *196*, 110. [CrossRef]
93. Wang, Z.; Lyu, H.; Zhang, C. Urban pluvial flood susceptibility mapping based on a novel explainable machine learning model with synchronous enhancement of fitting capability and explainability. *J. Hydrol.* **2024**, *642*, 131903. [CrossRef]
94. Shah, R.K.; Shah, R.K. GIS-based flood susceptibility analysis using multi-parametric approach of analytical hierarchy process in Majuli Island, Assam, India. *Sustain. Water Resour. Manag.* **2023**, *9*, 139. [CrossRef]
95. Hong, H.; Panahi, M.; Shirzadi, A.; Ma, T.; Liu, J.; Zhu, A.-X.; Chen, W.; Kougias, I.; Kazakis, N. Flood susceptibility assessment in Hengfeng area coupling adaptive neuro-fuzzy inference system with genetic algorithm and differential evolution. *Sci. Total Environ.* **2018**, *621*, 1124–1141. [CrossRef]
96. Tien Bui, D.; Khosravi, K.; Shahabi, H.; Daggupati, P.; Adamowski, J.F.; Melesse, A.M.; Thai Pham, B.; Pourghasemi, H.R.; Mahmoudi, M.; Bahrami, S. Flood spatial modeling in northern Iran using remote sensing and gis: A comparison between evidential belief functions and its ensemble with a multivariate logistic regression model. *Remote Sens.* **2019**, *11*, 1589. [CrossRef]
97. Saravanan, S.; Abijith, D. Flood susceptibility mapping of Northeast coastal districts of Tamil Nadu India using Multi-source Geospatial data and Machine Learning techniques. *Geocarto Int.* **2022**, *37*, 15252–15281. [CrossRef]
98. Danso, S.Y.; Ma, Y.; Osman, A.; Addo, I.Y. Integrating multi-criteria analysis and geospatial applications for mapping flood hazards in Sekondi-Takoradi Metropolis, Ghana. *J. Afr. Earth Sci.* **2024**, *209*, 105102. [CrossRef]
99. Li, W.; Liu, Y.; Liu, Z.; Gao, Z.; Huang, H.; Huang, W. A positive-unlabeled learning algorithm for urban flood susceptibility modeling. *Land* **2022**, *11*, 1971. [CrossRef]
100. Hussain, M.; Tayyab, M.; Ullah, K.; Ullah, S.; Rahman, Z.U.; Zhang, J.; Al-Shaibah, B. Development of a new integrated flood resilience model using machine learning with GIS-based multi-criteria decision analysis. *Urban Clim.* **2023**, *50*, 101589. [CrossRef]
101. Mokhtari, E.; Abdelkebir, B.; Djenaoui, A.; Hamdani, N.E.H. Integrated analytic hierarchy process and fuzzy analytic hierarchy process for Sahel watershed flood susceptibility assessment, Algeria. *Water Pract. Technol.* **2024**, *19*, 453–475. [CrossRef]
102. Aldiansyah, S.; Wardani, F. Evaluation of flood susceptibility prediction based on a resampling method using machine learning. *J. Water Clim. Change* **2023**, *14*, 937–961. [CrossRef]
103. Wu, Y.; She, D.; Xia, J.; Song, J.; Xiao, T.; Zhou, Y. The quantitative assessment of impact of pumping capacity and LID on urban flood susceptibility based on machine learning. *J. Hydrol.* **2023**, *617*, 129116. [CrossRef]
104. Wang, C.; Lin, Y.; Tao, Z.; Zhan, J.; Li, W.; Huang, H. An Inverse-Occurrence Sampling Approach for Urban Flood Susceptibility Mapping. *Remote Sens.* **2023**, *15*, 5384. [CrossRef]
105. Ren, H.; Pang, B.; Bai, P.; Zhao, G.; Liu, S.; Liu, Y.; Li, M. Flood Susceptibility Assessment with Random Sampling Strategy in Ensemble Learning (RF and XGBoost). *Remote Sens.* **2024**, *16*, 320. [CrossRef]
106. Khoirunisa, N.; Ku, C.-Y.; Liu, C.-Y. A GIS-based artificial neural network model for flood susceptibility assessment. *Int. J. Environ. Res. Public Health* **2021**, *18*, 1072. [CrossRef] [PubMed]

107. Saleh, A.; Yuzir, A.; Sabtu, N.; Abujayyab, S.K.; Bunmi, M.R.; Pham, Q.B. Flash flood susceptibility mapping in urban area using genetic algorithm and ensemble method. *Geocarto Int.* **2022**, *37*, 10199–10228. [CrossRef]
108. Lin, L.; Wu, Z.; Liang, Q. Urban flood susceptibility analysis using a GIS-based multi-criteria analysis framework. *Nat. Hazards* **2019**, *97*, 455–475. [CrossRef]
109. Fu, S.; Lyu, H.; Wang, Z.; Hao, X.; Zhang, C. Extracting historical flood locations from news media data by the named entity recognition (NER) model to assess urban flood susceptibility. *J. Hydrol.* **2022**, *612*, 128312. [CrossRef]
110. Zhao, G.; Pang, B.; Xu, Z.; Peng, D.; Xu, L. Assessment of urban flood susceptibility using semi-supervised machine learning model. *Sci. Total Environ.* **2019**, *659*, 940–949. [CrossRef]
111. Zhao, G.; Pang, B.; Xu, Z.; Peng, D.; Zuo, D. Urban flood susceptibility assessment based on convolutional neural networks. *J. Hydrol.* **2020**, *590*, 125235. [CrossRef]
112. Seleem, O.; Ayzel, G.; de Souza, A.C.T.; Bronstert, A.; Heistermann, M. Towards urban flood susceptibility mapping using data-driven models in Berlin, Germany. *Geomat. Nat. Hazards Risk* **2022**, *13*, 1640–1662. [CrossRef]
113. Yao, L.; Li, T.; Xu, M.; Xu, Y. How the landscape features of urban green space impact seasonal land surface temperatures at a city-block-scale: An urban heat island study in Beijing, China. *Urban For. Urban Green.* **2020**, *52*, 126704. [CrossRef]
114. Niyongabire, E.; Hassan, R.; Elhassan, E.; Mehdi, M. Use of digital elevation model in a GIS for flood susceptibility mapping: Case of Bujumbura City. In Proceedings of the 6th International Conference on Cartography and GIS, Albena, Bulgaria, 13–17 June 2016; pp. 241–248.
115. Zhao, J.; Zhang, C.; Wang, J.; Abbas, Z.; Zhao, Y. Machine learning and SHAP-based susceptibility assessment of storm flood in rapidly urbanizing areas: A case study of Shenzhen, China. *Geomat. Nat. Hazards Risk* **2024**, *15*, 2311889. [CrossRef]
116. Boulomytis, V.T.G.; Zuffo, A.C.; Imteaz, M.A. Assessment of flood susceptibility in coastal peri-urban areas: An alternative MCDA approach for ungauged catchments. *Urban Water J.* **2022**, *21*, 1022–1034. [CrossRef]
117. Hammami, S.; Zouhri, L.; Souissi, D.; Souei, A.; Zghibi, A.; Marzougui, A.; Dlala, M. Application of the GIS based multi-criteria decision analysis and analytical hierarchy process (AHP) in the flood susceptibility mapping (Tunisia). *Arab. J. Geosci.* **2019**, *12*, 653. [CrossRef]
118. Chaulagain, D.; Rimal, P.R.; Ngando, S.N.; Nsafon, B.E.K.; Suh, D.; Huh, J.-S. Flood susceptibility mapping of Kathmandu metropolitan city using GIS-based multi-criteria decision analysis. *Ecol. Indic.* **2023**, *154*, 110653. [CrossRef]
119. Panfilova, T.; Kukartsev, V.; Tynchenko, V.; Tynchenko, Y.; Kukartseva, O.; Kleshko, I.; Wu, X.; Malashin, I. Flood susceptibility assessment in urban areas via deep neural network approach. *Sustainability* **2024**, *16*, 7489. [CrossRef]
120. Chen, Y.; Ye, Z.; Liu, H.; Chen, R.; Liu, Z. A GIS-based approach for flood risk zoning by combining social vulnerability and flood susceptibility: A case study of Nanjing, China. *Int. J. Environ. Res. Public Health* **2021**, *18*, 11597. [CrossRef]
121. Ajibade, F.O.; Ajibade, T.F.; Idowu, T.E.; Nwogwu, N.A.; Adelodun, B.; Lasisi, K.H.; Opafola, O.T.; Ajala, O.A.; Fadugba, O.G.; Adewumi, J.R. Flood-prone area mapping using GIS-based analytical hierarchy frameworks for Ibadan city, Nigeria. *J. Multi-Criteria Decis. Anal.* **2021**, *28*, 283–295. [CrossRef]
122. Malekinezhad, H.; Sepehri, M.; Pham, Q.B.; Hosseini, S.Z.; Meshram, S.G.; Vojtek, M.; Vojteková, J. Application of entropy weighting method for urban flood hazard mapping. *Acta Geophys.* **2021**, *69*, 841–854. [CrossRef]
123. Fang, J.; Zhang, C.; Fang, J.; Liu, M.; Luan, Y. Increasing exposure to floods in China revealed by nighttime light data and flood susceptibility mapping. *Environ. Res. Lett.* **2021**, *16*, 104044. [CrossRef]
124. Esfandiari, M.; Jabari, S.; McGrath, H.; Coleman, D. Flood mapping using random forest and identifying the essential conditioning factors; a case study in Fredericton, New Brunswick, Canada. *ISPRS Ann. Photogramm. Remote Sens. Spat. Inf. Sci.* **2020**, *3*, 609–615. [CrossRef]
125. Sozer, B.; Kocaman, S.; Nefeslioglu, H.A.; Firat, O.; Gokceoglu, C. Preliminary investigations on flood susceptibility mapping in Ankara (Turkey) using modified analytical hierarchy process (M-AHP). *Int. Arch. Photogramm. Remote Sens. Spat. Inf. Sci.* **2018**, *42*, 361–365. [CrossRef]
126. Vaddiraju, S.C.; Talari, R. Urban flood susceptibility analysis of Saroor Nagar Watershed of India using Geomatics-based multi-criteria analysis framework. *Environ. Sci. Pollut. Res.* **2023**, *30*, 107021–107040. [CrossRef]
127. Stamellou, E.; Kalogeropoulos, K.; Stathopoulos, N.; Tsesmelis, D.E.; Louka, P.; Apostolidis, V.; Tsatsaris, A. A GIS-cellular automata-based model for coupling urban sprawl and flood susceptibility assessment. *Hydrology* **2021**, *8*, 159. [CrossRef]
128. Alves, M.L.P.R.; Oliveira, R.G.L.; Rocha, C.A.A.; Filgueira, H.J.A.; da Silva, R.M.; Santos, C.A.G. Assessing flood susceptibility with ALOS PALSAR and LiDAR digital terrain models using the height above nearest drainage (HAND) model. *Environ. Dev. Sustain.* **2024**, 1–24. [CrossRef]
129. Jato-Espino, D.; Lobo, A.; Ascorbe-Salcedo, A. Urban flood risk mapping using an optimised additive weighting methodology based on open data. *J. Flood Risk Manag.* **2019**, *12*, e12533. [CrossRef]
130. Swathika, R.; Radha, N.; Sasirekha, S.; Dhanabal, S. Flood susceptibility in urban environment using multi-layered neural network model from satellite imagery sources. *Glob. NEST J.* **2023**, *25*, 60–73.

131. Amiri, A.; Soltani, K.; Ebtehaj, I.; Bonakdari, H. A novel machine learning tool for current and future flood susceptibility mapping by integrating remote sensing and geographic information systems. *J. Hydrol.* **2024**, *632*, 130936. [CrossRef]
132. Ullah, K.; Zhang, J. GIS-based flood hazard mapping using relative frequency ratio method: A case study of Panjkora River Basin, eastern Hindu Kush, Pakistan. *PLoS ONE* **2020**, *15*, e0229153. [CrossRef]
133. Sahana, M.; Patel, P.P. A comparison of frequency ratio and fuzzy logic models for flood susceptibility assessment of the lower Kosi River Basin in India. *Environ. Earth Sci.* **2019**, *78*, 289. [CrossRef]
134. Waqas, H.; Lu, L.; Tariq, A.; Li, Q.; Baqa, M.F.; Xing, J.; Sajjad, A. Flash flood susceptibility assessment and zonation using an integrating analytic hierarchy process and frequency ratio model for the Chitral District, Khyber Pakhtunkhwa, Pakistan. *Water* **2021**, *13*, 1650. [CrossRef]
135. Liuzzo, L.; Sammartano, V.; Freni, G. Comparison between different distributed methods for flood susceptibility mapping. *Water Resour. Manag.* **2019**, *33*, 3155–3173. [CrossRef]
136. O'Donnell, E.C.; Thorne, C.R. Drivers of future urban flood risk. *Philos. Trans. R. Soc. A* **2020**, *378*, 20190216. [CrossRef]
137. Zhang, H.; Jia, H.; Li, C.; Zhang, Q. Exploring the driving factors of urban flood at the catchment Scale: A case study of multitype megacities in China. *Ecol. Indic.* **2024**, *166*, 112513. [CrossRef]
138. Ilderomi, A.R.; Vojtek, M.; Vojteková, J.; Pham, Q.B.; Kuriqi, A.; Sepehri, M. Flood prioritization integrating picture fuzzy-analytic hierarchy and fuzzy-linear assignment model. *Arab. J. Geosci.* **2022**, *15*, 1185. [CrossRef]
139. Nguyen, H.D. Spatial modeling of flood hazard using machine learning and GIS in Ha Tinh province, Vietnam. *J. Water Clim. Change* **2023**, *14*, 200–222. [CrossRef]
140. Ruidas, D.; Chakrabortty, R.; Islam, A.R.M.T.; Saha, A.; Pal, S.C. A novel hybrid of meta-optimization approach for flash flood-susceptibility assessment in a monsoon-dominated watershed, Eastern India. *Environ. Earth Sci.* **2022**, *81*, 145. [CrossRef]
141. Siahkamari, S.; Haghizadeh, A.; Zeinivand, H.; Tahmasebipour, N.; Rahmati, O. Spatial prediction of flood-susceptible areas using frequency ratio and maximum entropy models. *Geocarto Int.* **2018**, *33*, 927–941. [CrossRef]
142. Tehrany, M.S.; Pradhan, B.; Jebur, M.N. Flood susceptibility analysis and its verification using a novel ensemble support vector machine and frequency ratio method. *Stoch. Environ. Res. Risk Assess.* **2015**, *29*, 1149–1165. [CrossRef]
143. Khosravi, K.; Nohani, E.; Maroufinia, E.; Pourghasemi, H.R. A GIS-based flood susceptibility assessment and its mapping in Iran: A comparison between frequency ratio and weights-of-evidence bivariate statistical models with multi-criteria decision-making technique. *Nat. Hazards* **2016**, *83*, 947–987. [CrossRef]
144. Khosravi, K.; Shahabi, H.; Pham, B.T.; Adamowski, J.; Shirzadi, A.; Pradhan, B.; Dou, J.; Ly, H.-B.; Gróf, G.; Ho, H.L. A comparative assessment of flood susceptibility modeling using multi-criteria decision-making analysis and machine learning methods. *J. Hydrol.* **2019**, *573*, 311–323. [CrossRef]
145. Zhao, G.; Pang, B.; Xu, Z.; Yue, J.; Tu, T. Mapping flood susceptibility in mountainous areas on a national scale in China. *Sci. Total Environ.* **2018**, *615*, 1133–1142. [CrossRef]
146. Gaurkhede, N.; Adane, V. Flood Susceptibility Analysis Using Freely Available Data, Gis, and Frequency Ratio Model for Nagpur, India. *Appl. Ecol. Environ. Res.* **2023**, *21*, 2341–2361. [CrossRef]
147. Li, Y.; Osei, F.B.; Hu, T.; Stein, A. Urban flood susceptibility mapping based on social media data in Chengdu city, China. *Sustain. Cities Soc.* **2023**, *88*, 104307. [CrossRef]
148. Darabi, H.; Rahmati, O.; Naghibi, S.A.; Mohammadi, F.; Ahmadisharaf, E.; Kalantari, Z.; Torabi Haghighi, A.; Soleimanpour, S.M.; Tiefenbacher, J.P.; Tien Bui, D. Development of a novel hybrid multi-boosting neural network model for spatial prediction of urban flood. *Geocarto Int.* **2022**, *37*, 5716–5741. [CrossRef]
149. Dutal, H. Determining the effect of urbanization on flood hazard zones in Kahramanmaras, Turkey, using flood hazard index and multi-criteria decision analysis. *Environ. Monit. Assess.* **2023**, *195*, 92. [CrossRef]
150. Bouamrane, A.; Derdous, O.; Dahri, N.; Tachi, S.-E.; Boutebba, K.; Bouziane, M.T. A comparison of the analytical hierarchy process and the fuzzy logic approach for flood susceptibility mapping in a semi-arid ungauged basin (Biskra basin: Algeria). *Int. J. River Basin Manag.* **2022**, *20*, 203–213. [CrossRef]
151. Bagyaraj, M.; Senapathi, V.; Chung, S.Y.; Gopalakrishnan, G.; Xiao, Y.; Karthikeyan, S.; Nadiri, A.A.; Barzegar, R. A geospatial approach for assessing urban flood risk zones in Chennai, Tamil Nadu, India. *Environ. Sci. Pollut. Res.* **2023**, *30*, 100562–100575. [CrossRef]
152. Khouz, A.; Trindade, J.; Santos, P.P.; Oliveira, S.C.; El Bchari, F.; Bougadir, B.; Garcia, R.A.; Reis, E.; Jadoud, M.; Saouabe, T. Flood susceptibility assessment through statistical models and HEC-RAS analysis for sustainable management in Essaouira Province, Morocco. *Geosciences* **2023**, *13*, 382. [CrossRef]
153. Falah, F.; Rahmati, O.; Rostami, M.; Ahmadisharaf, E.; Daliakopoulos, I.N.; Pourghasemi, H.R. Artificial neural networks for flood susceptibility mapping in data-scarce urban areas. In *Spatial Modeling in GIS and R for Earth and Environmental Sciences*; Elsevier: Amsterdam, The Netherlands, 2019; pp. 323–336.
154. Luo, Z.; Tian, J.; Zeng, J.; Pilla, F. Resilient landscape pattern for reducing coastal flood susceptibility. *Sci. Total Environ.* **2023**, *856*, 159087. [CrossRef]

155. Lee, S.; Lee, S.; Lee, M.-J.; Jung, H.-S. Spatial assessment of urban flood susceptibility using data mining and geographic information System (GIS) tools. *Sustainability* **2018**, *10*, 648. [CrossRef]
156. Lee, S.; Kim, J.-C.; Jung, H.-S.; Lee, M.J.; Lee, S. Spatial prediction of flood susceptibility using random-forest and boosted-tree models in Seoul metropolitan city, Korea. *Geomat. Nat. Hazards Risk* **2017**, *8*, 1185–1203. [CrossRef]
157. Ouma, Y.O.; Omai, L. Flood Susceptibility Mapping Using Image-Based 2D-CNN Deep Learning: Overview and Case Study Application Using Multiparametric Spatial Data in Data-Scarce Urban Environments. *Int. J. Intell. Syst.* **2023**, *2023*, 5672401. [CrossRef]
158. Di Salvo, C.; Pennica, F.; Ciotoli, G.; Cavinato, G.P. A GIS-based procedure for preliminary mapping of pluvial flood risk at metropolitan scale. *Environ. Model. Softw.* **2018**, *107*, 64–84. [CrossRef]
159. Madhuri, R.; Srinivasa Raju, K.; Vasan, A. Flood-susceptibility-based building risk under climate change, Hyderabad, India. *J. Water Clim. Change* **2023**, *14*, 2150–2163. [CrossRef]
160. Nachappa, T.G.; Piralilou, S.T.; Gholamnia, K.; Ghorbanzadeh, O.; Rahmati, O.; Blaschke, T. Flood susceptibility mapping with machine learning, multi-criteria decision analysis and ensemble using Dempster Shafer Theory. *J. Hydrol.* **2020**, *590*, 125275. [CrossRef]
161. Rahman, M.; Ningsheng, C.; Islam, M.M.; Dewan, A.; Iqbal, J.; Washakh, R.M.A.; Shufeng, T. Flood susceptibility assessment in Bangladesh using machine learning and multi-criteria decision analysis. *Earth Syst. Environ.* **2019**, *3*, 585–601. [CrossRef]
162. Hosseini Sabzevari, S.A.; Mehdipour, H.; Aslani, F. An assessment of flash flood susceptibility in Golestan province, Iran, using multiple computational approaches. *Int. J. Disaster Resil. Built Environ.* **2024**, *15*, 341–356. [CrossRef]
163. Tehrany, M.S.; Pradhan, B.; Jebur, M.N. Flood susceptibility mapping using a novel ensemble weights-of-evidence and support vector machine models in GIS. *J. Hydrol.* **2014**, *512*, 332–343. [CrossRef]
164. Li, S.; Wang, Z.; Lai, C.; Lin, G. Quantitative assessment of the relative impacts of climate change and human activity on flood susceptibility based on a cloud model. *J. Hydrol.* **2020**, *588*, 125051. [CrossRef]
165. Salami, H.S.; Otokiti, K.V. Ineffective development control and flood susceptibility in Lokoja, Nigeria. *Discovery* **2019**, *55*, 468–476.
166. Warlina, L.; Guinensa, F. Flood susceptibility and spatial analysis of pangkalpinang city, bangka belitung, indonesia. *J. Eng. Sci. Technol.* **2019**, *14*, 3481–3495.
167. Lee, M.-J.; Kang, J.-e.; Jeon, S. Application of frequency ratio model and validation for predictive flooded area susceptibility mapping using GIS. In Proceedings of the 2012 IEEE International Geoscience and Remote Sensing Symposium, Munich, Germany, 22–27 July 2012; pp. 895–898.
168. Hong, H.; Tsangaratos, P.; Ilia, I.; Liu, J.; Zhu, A.-X.; Chen, W. Application of fuzzy weight of evidence and data mining techniques in construction of flood susceptibility map of Poyang County, China. *Sci. Total Environ.* **2018**, *625*, 575–588. [CrossRef]
169. Al-Juaidi, A.E.; Nassar, A.M.; Al-Juaidi, O.E. Evaluation of flood susceptibility mapping using logistic regression and GIS conditioning factors. *Arab. J. Geosci.* **2018**, *11*, 765. [CrossRef]
170. Pandey, D.; Singh, K.K. Comparison of Urban Flood Susceptibility Maps of MIKE+ and AHP with GIS Integration: A Case Study of Rohtak City, India. In Proceedings of the World Environmental and Water Resources Congress, Milwaukee, WI, USA, 19–22 May 2024; pp. 659–672.
171. Guimarães da Silva, L.; de Souza Catelani, C.; dos Santos Targa, M. Analytic hierarchy process (AHP) applied to flood susceptibility in São José dos Campos, São Paulo, Brazil. *Rev. Ambiente E Água* **2020**, *15*, 1. [CrossRef]
172. Mahmoud, S.H.; Gan, T.Y. Multi-criteria approach to develop flood susceptibility maps in arid regions of Middle East. *J. Clean. Prod.* **2018**, *196*, 216–229. [CrossRef]
173. Swain, K.C.; Singha, C.; Nayak, L. Flood susceptibility mapping through the GIS-AHP technique using the cloud. *ISPRS Int. J. Geo-Inf.* **2020**, *9*, 720. [CrossRef]
174. Bui, D.T.; Pradhan, B.; Nampak, H.; Bui, Q.-T.; Tran, Q.-A.; Nguyen, Q.-P. Hybrid artificial intelligence approach based on neural fuzzy inference model and metaheuristic optimization for flood susceptibilitgy modeling in a high-frequency tropical cyclone area using GIS. *J. Hydrol.* **2016**, *540*, 317–330.
175. Zhao, G.; Pang, B.; Xu, Z.; Cui, L.; Wang, J.; Zuo, D.; Peng, D. Improving urban flood susceptibility mapping using transfer learning. *J. Hydrol.* **2021**, *602*, 126777. [CrossRef]
176. Mind'je, R.; Li, L.; Amanambu, A.C.; Nahayo, L.; Nsengiyumva, J.B.; Gasirabo, A.; Mindje, M. Flood susceptibility modeling and hazard perception in Rwanda. *Int. J. Disaster Risk Reduct.* **2019**, *38*, 101211. [CrossRef]
177. Wang, M.; Li, Y.; Yuan, H.; Zhou, S.; Wang, Y.; Ikram, R.M.A.; Li, J. An XGBoost-SHAP approach to quantifying morphological impact on urban flooding susceptibility. *Ecol. Indic.* **2023**, *156*, 111137. [CrossRef]
178. Rafiei-Sardooi, E.; Azareh, A.; Choubin, B.; Mosavi, A.H.; Clague, J.J. Evaluating urban flood risk using hybrid method of TOPSIS and machine learning. *Int. J. Disaster Risk Reduct.* **2021**, *66*, 102614. [CrossRef]
179. Wang, H.; Meng, Y.; Wang, H.; Wu, Z.; Guan, X. The application of integrating comprehensive evaluation and clustering algorithms weighted by maximal information coefficient for urban flood susceptibility. *J. Environ. Manag.* **2023**, *344*, 118846. [CrossRef]

180. Bouamrane, A.; Derdous, O.; Bouchehed, H.; Abida, H. Assessing future changes in flood susceptibility under projections from the sixth coupled model intercomparison project: Case study of Algiers City (Algeria). *Nat. Hazards* **2024**, 1–21. [CrossRef]
181. Rahmati, O.; Darabi, H.; Panahi, M.; Kalantari, Z.; Naghibi, S.A.; Ferreira, C.S.S.; Kornejady, A.; Karimidastenaei, Z.; Mohammadi, F.; Stefanidis, S. Development of novel hybridized models for urban flood susceptibility mapping. *Sci. Rep.* **2020**, *10*, 12937. [CrossRef] [PubMed]
182. Sarkadi, N.; Pirkhoffer, E.; Lóczy, D.; Balatonyi, L.; Geresdi, I.; Fábián, S.Á.; Varga, G.; Balogh, R.; Gradwohl-Valkay, A.; Halmai, Á. Generation of a flood susceptibility map of evenly weighted conditioning factors for Hungary. *Geogr. Pannonica* **2022**, *26*, 200–214. [CrossRef]
183. Tang, Z.; Zhang, H.; Yi, S.; Xiao, Y. Assessment of flood susceptible areas using spatially explicit, probabilistic multi-criteria decision analysis. *J. Hydrol.* **2018**, *558*, 144–158. [CrossRef]
184. El-Haddad, B.A.; Youssef, A.M.; Pourghasemi, H.R.; Pradhan, B.; El-Shater, A.-H.; El-Khashab, M.H. Flood susceptibility prediction using four machine learning techniques and comparison of their performance at Wadi Qena Basin, Egypt. *Nat. Hazards* **2021**, *105*, 83–114. [CrossRef]
185. Baalousha, H.M.; Tawabini, B.; Bokhari, B. A fuzzy analytical hierarchy process-GIS approach to flood susceptibility mapping in NEOM, Saudi Arabia. *Front. Water* **2024**, *6*, 1388003.
186. Shirzadi, B.; Veisi, F.; Ghorbani, M.S.; Shirzadi, A.; Shahabi, H. Urban flood susceptibility prediction using a Fuzzy-Delphi hybrid model in Sanandaj City. *Water Soil Manag. Model.* **2024**, *4*, 143–158.
187. Rezaei, M.; Amiraslani, F.; Samani, N.N.; Alavipanah, K. Application of two fuzzy models using knowledge-based and linear aggregation approaches to identifying flooding-prone areas in Tehran. *Nat. Hazards* **2020**, *100*, 363–385. [CrossRef]
188. Mukherjee, F.; Singh, D. Detecting flood prone areas in Harris County: A GIS based analysis. *GeoJournal* **2020**, *85*, 647–663. [CrossRef]
189. Cikmaz, B.; Yildirim, E.; Demir, I. Flood susceptibility mapping using fuzzy analytical hierarchy process for Cedar Rapids, Iowa. *EarthArxiv* **2022**. [CrossRef]
190. Corapci, F.; Ozdemir, H. A new approach to flood susceptibility analysis of urbanised alluvial fans: The case of Bursa City (Türkiye). *Nat. Hazards* **2024**, *120*, 12909–12932. [CrossRef]
191. Wang, Z.; Lyu, H.; Zhang, C. Pluvial flood susceptibility mapping for data-scarce urban areas using graph attention network and basic flood conditioning factors. *Geocarto Int.* **2023**, *38*, 2275692. [CrossRef]
192. Morelli, S.; Battistini, A.; Catani, F. Rapid assessment of flood susceptibility in urbanized rivers using digital terrain data: Application to the Arno river case study (Firenze, northern Italy). *Appl. Geogr.* **2014**, *54*, 35–53. [CrossRef]
193. Qi, W.; Ma, C.; Xu, H.; Chen, Z.; Zhao, K.; Han, H. A review on applications of urban flood models in flood mitigation strategies. *Nat. Hazards* **2021**, *108*, 31–62. [CrossRef]
194. Song, J.; Shao, Z.; Zhan, Z.; Chen, L. State-of-the-Art Techniques for Real-Time Monitoring of Urban Flooding: A Review. *Water* **2024**, *16*, 2476. [CrossRef]
195. Luo, P.; Luo, M.; Li, F.; Qi, X.; Huo, A.; Wang, Z.; He, B.; Takara, K.; Nover, D.; Wang, Y. Urban flood numerical simulation: Research, methods and future perspectives. *Environ. Model. Softw.* **2022**, *156*, 105478. [CrossRef]
196. Sun, H.; Zhang, X.; Ruan, X.; Jiang, H.; Shou, W. Mapping Compound Flooding Risks for Urban Resilience in Coastal Zones: A Comprehensive Methodological Review. *Remote Sens.* **2024**, *16*, 350. [CrossRef]
197. Samanta, R.K.; Bhunia, G.S.; Shit, P.K.; Pourghasemi, H.R. Flood susceptibility mapping using geospatial frequency ratio technique: A case study of Subarnarekha River Basin, India. *Model. Earth Syst. Environ.* **2018**, *4*, 395–408. [CrossRef]
198. Cao, C.; Xu, P.; Wang, Y.; Chen, J.; Zheng, L.; Niu, C. Flash flood hazard susceptibility mapping using frequency ratio and statistical index methods in coalmine subsidence areas. *Sustainability* **2016**, *8*, 948. [CrossRef]
199. Liu, J.; Wang, J.; Xiong, J.; Cheng, W.; Li, Y.; Cao, Y.; He, Y.; Duan, Y.; He, W.; Yang, G. Assessment of flood susceptibility mapping using support vector machine, logistic regression and their ensemble techniques in the Belt and Road region. *Geocarto Int.* **2022**, *37*, 9817–9846. [CrossRef]
200. Rahmati, O.; Pourghasemi, H.R.; Zeinivand, H. Flood susceptibility mapping using frequency ratio and weights-of-evidence models in the Golastan Province, Iran. *Geocarto Int.* **2016**, *31*, 42–70. [CrossRef]
201. Shikhteymour, S.R.; Borji, M.; Bagheri-Gavkosh, M.; Azimi, E.; Collins, T.W. A novel approach for assessing flood risk with machine learning and multi-criteria decision-making methods. *Appl. Geogr.* **2023**, *158*, 103035. [CrossRef]
202. Ekmekcioğlu, Ö.; Koc, K.; Özger, M. District based flood risk assessment in Istanbul using fuzzy analytical hierarchy process. *Stoch. Environ. Res. Risk Assess.* **2021**, *35*, 617–637. [CrossRef]
203. Eini, M.; Kaboli, H.S.; Rashidian, M.; Hedayat, H. Hazard and vulnerability in urban flood risk mapping: Machine learning techniques and considering the role of urban districts. *Int. J. Disaster Risk Reduct.* **2020**, *50*, 101687. [CrossRef]
204. Tehrany, M.S.; Lee, M.-J.; Pradhan, B.; Jebur, M.N.; Lee, S. Flood susceptibility mapping using integrated bivariate and multivariate statistical models. *Environ. Earth Sci.* **2014**, *72*, 4001–4015. [CrossRef]

205. Lyu, H.-M.; Shen, S.-L.; Zhou, A.; Yang, J. Perspectives for flood risk assessment and management for mega-city metro system. *Tunn. Undergr. Space Technol.* **2019**, *84*, 31–44. [CrossRef]
206. Hou, J.; Zhou, N.; Chen, G.; Huang, M.; Bai, G. Rapid forecasting of urban flood inundation using multiple machine learning models. *Nat. Hazards* **2021**, *108*, 2335–2356. [CrossRef]
207. Bathrellos, G.D.; Karymbalis, E.; Skilodimou, H.D.; Gaki-Papanastassiou, K.; Baltas, E.A. Urban flood hazard assessment in the basin of Athens Metropolitan city, Greece. *Environ. Earth Sci.* **2016**, *75*, 319. [CrossRef]
208. Msaddek, M.H.; Merzougui, A.; Zghibi, A.; Chekirbane, A. Integrated decisional approach for watershed vulnerability prioritization using water and soil hazard index (WSHI) and AHP methods: Chiba watershed, Cap-Bon region, northeast Tunisia. *Arab. J. Geosci.* **2022**, *15*, 1148. [CrossRef]
209. Seejata, K.; Yodying, A.; Wongthadam, T.; Mahavik, N.; Tantanee, S. Assessment of flood hazard areas using analytical hierarchy process over the Lower Yom Basin, Sukhothai Province. *Procedia Eng.* **2018**, *212*, 340–347. [CrossRef]
210. Souissi, D.; Zouhri, L.; Hammami, S.; Msaddek, M.H.; Zghibi, A.; Dlala, M. GIS-based MCDM–AHP modeling for flood susceptibility mapping of arid areas, southeastern Tunisia. *Geocarto Int.* **2020**, *35*, 991–1017. [CrossRef]
211. Gupta, L.; Dixit, J. A GIS-based flood risk mapping of Assam, India, using the MCDA-AHP approach at the regional and administrative level. *Geocarto Int.* **2022**, *37*, 11867–11899. [CrossRef]
212. Sharma, N.; Goswami, J.; Sharma, P. Utilisation of Geo-Spatial Technology to Study the Variation in Access of Urban Health Care Centres in Kamrup Metropolitan, Assam, India. In *Geospatial Technology and Smart Cities: ICT, Geoscience Modeling, GIS and Remote Sensing*; Springer: Berlin/Heidelberg, Germany, 2021; pp. 203–224.
213. Bera, S.; Das, A.; Mazumder, T. Evaluation of machine learning, information theory and multi-criteria decision analysis methods for flood susceptibility mapping under varying spatial scale of analyses. *Remote Sens. Appl. Soc. Environ.* **2022**, *25*, 100686. [CrossRef]
214. El baida, M.; Hosni, M.; Boushaba, F.; Chourak, M. A systematic literature review on classification machine learning for urban flood hazard mapping. *Water Resour. Manag.* **2024**, *38*, 5823–5864. [CrossRef]
215. Pourghasemi, H.R.; Amiri, M.; Edalat, M.; Ahrari, A.H.; Panahi, M.; Sadhasivam, N.; Lee, S. Assessment of urban infrastructures exposed to flood using susceptibility map and Google Earth Engine. *IEEE J. Sel. Top. Appl. Earth Obs. Remote Sens.* **2020**, *14*, 1923–1937. [CrossRef]
216. Motta, M.; de Castro Neto, M.; Sarmento, P. A mixed approach for urban flood prediction using Machine Learning and GIS. *Int. J. Disaster Risk Reduct.* **2021**, *56*, 102154. [CrossRef]
217. Parvin, F.; Ali, S.A.; Calka, B.; Bielecka, E.; Linh, N.T.T.; Pham, Q.B. Urban flood vulnerability assessment in a densely urbanized city using multi-factor analysis and machine learning algorithms. *Theor. Appl. Climatol.* **2022**, *149*, 639–659. [CrossRef]
218. Fang, Z.; Wang, Y.; Peng, L.; Hong, H. Predicting flood susceptibility using LSTM neural networks. *J. Hydrol.* **2021**, *594*, 125734. [CrossRef]
219. Chen, W.; Li, Y.; Xue, W.; Shahabi, H.; Li, S.; Hong, H.; Wang, X.; Bian, H.; Zhang, S.; Pradhan, B. Modeling flood susceptibility using data-driven approaches of naïve bayes tree, alternating decision tree, and random forest methods. *Sci. Total Environ.* **2020**, *701*, 134979. [CrossRef]
220. Band, S.S.; Janizadeh, S.; Chandra Pal, S.; Saha, A.; Chakrabortty, R.; Melesse, A.M.; Mosavi, A. Flash flood susceptibility modeling using new approaches of hybrid and ensemble tree-based machine learning algorithms. *Remote Sens.* **2020**, *12*, 3568. [CrossRef]
221. Roy, P.; Pal, S.C.; Chakrabortty, R.; Chowdhuri, I.; Malik, S.; Das, B. Threats of climate and land use change on future flood susceptibility. *J. Clean. Prod.* **2020**, *272*, 122757. [CrossRef]
222. Giovannettone, J.; Copenhaver, T.; Burns, M.; Choquette, S. A statistical approach to mapping flood susceptibility in the Lower Connecticut River Valley Region. *Water Resour. Res.* **2018**, *54*, 7603–7618. [CrossRef]
223. Abedi, R.; Costache, R.; Shafizadeh-Moghadam, H.; Pham, Q.B. Flash-flood susceptibility mapping based on XGBoost, random forest and boosted regression trees. *Geocarto Int.* **2022**, *37*, 5479–5496. [CrossRef]
224. Kohansarbaz, A.; Kohansarbaz, A.; Shabanlou, S.; Yosefvand, F.; Rajabi, A. Modelling flood susceptibility in northern Iran: Application of five well-known machine-learning models. *Irrig. Drain.* **2022**, *71*, 1332–1350. [CrossRef]
225. Agonafir, C.; Lakhankar, T.; Khanbilvardi, R.; Krakauer, N.; Radell, D.; Devineni, N. A machine learning approach to evaluate the spatial variability of New York City's 311 street flooding complaints. *Comput. Environ. Urban Syst.* **2022**, *97*, 101854. [CrossRef]
226. Norallahi, M.; Seyed Kaboli, H. Urban flood hazard mapping using machine learning models: GARP, RF, MaxEnt and NB. *Nat. Hazards* **2021**, *106*, 119–137. [CrossRef]
227. Kilsdonk, R.A.; Bomers, A.; Wijnberg, K.M. Predicting urban flooding due to extreme precipitation using a long short-term memory neural network. *Hydrology* **2022**, *9*, 105. [CrossRef]
228. Ekwueme, B.N. Machine learning based prediction of urban flood susceptibility from selected rivers in a tropical catchment area. *Civ. Eng. J.* **2022**, *8*, 1857. [CrossRef]
229. Chen, J.; Huang, G.; Chen, W. Towards better flood risk management: Assessing flood risk and investigating the potential mechanism based on machine learning models. *J. Environ. Manag.* **2021**, *293*, 112810. [CrossRef]

230. Shah, A.G.; Nakhuda, M.S.; Kumar, S.; Vincent, S.; Kumar, O.P. Machine Learning for Flood Susceptibility Mapping of the Chennai Floods of 2023. In Proceedings of the 2024 IEEE International Conference on Signal Processing, Informatics, Communication and Energy Systems (SPICES), Kottayam, India, 20–22 September 2024; pp. 1–6.
231. Nguyen, H.D. GIS-based hybrid machine learning for flood susceptibility prediction in the Nhat Le–Kien Giang watershed, Vietnam. *Earth Sci. Inform.* **2022**, *15*, 2369–2386. [CrossRef]
232. Asfaw, W.; Rientjes, T.; Bekele, T.W.; Haile, A.T. Estimating Elements Susceptible to Urban Flooding Using Multisource Data and Machine Learning. *Int. J. Disaster Risk Reduct.* **2024**, *116*, 105169. [CrossRef]
233. Szeląg, B.; Majerek, D.; Eusebi, A.L.; Kiczko, A.; de Paola, F.; McGarity, A.; Wałek, G.; Fatone, F. Tool for fast assessment of stormwater flood volumes for urban catchment: A machine learning approach. *J. Environ. Manag.* **2024**, *355*, 120214. [CrossRef] [PubMed]
234. Costache, R.; Arabameri, A.; Costache, I.; Crăciun, A.; Pham, B.T. New machine learning ensemble for flood susceptibility estimation. *Water Resour. Manag.* **2022**, *36*, 4765–4783. [CrossRef]
235. Kalantar, B.; Ueda, N.; Saeidi, V.; Janizadeh, S.; Shabani, F.; Ahmadi, K.; Shabani, F. Deep neural network utilizing remote sensing datasets for flood hazard susceptibility mapping in Brisbane, Australia. *Remote Sens.* **2021**, *13*, 2638. [CrossRef]
236. Tehrany, M.S.; Kumar, L.; Shabani, F. A novel GIS-based ensemble technique for flood susceptibility mapping using evidential belief function and support vector machine: Brisbane, Australia. *PeerJ* **2019**, *7*, e7653. [CrossRef]
237. Wubalem, A.; Tesfaw, G.; Dawit, Z.; Getahun, B.; Mekuria, T.; Jothimani, M. Comparison of statistical and analytical hierarchy process methods on flood susceptibility mapping: In a case study of the Lake Tana sub-basin in northwestern Ethiopia. *Open Geosci.* **2021**, *13*, 1668–1688. [CrossRef]
238. Zhao, H.; Yao, L.; Mei, G.; Liu, T.; Ning, Y. A fuzzy comprehensive evaluation method based on AHP and entropy for a landslide susceptibility map. *Entropy* **2017**, *19*, 396. [CrossRef]
239. Nkwunonwo, U.; Whitworth, M.; Baily, B. A review of the current status of flood modelling for urban flood risk management in the developing countries. *Sci. Afr.* **2020**, *7*, e00269. [CrossRef]
240. Liu, C.; Hu, C.; Zhao, C.; Sun, Y.; Xie, T.; Wang, H. Research on Urban Storm Flood Simulation by Coupling K-means Machine Learning Algorithm and GIS Spatial Analysis Technology into SWMM Model. *Water Resour. Manag.* **2024**, *38*, 2059–2078. [CrossRef]
241. Géron, A. *Hands-on Machine Learning with Scikit-Learn, Keras, and Tensor Flow*; O'Reilly Media, Inc.: Sebastopol, CA, USA, 2022.
242. Xu, K.; Han, Z.; Xu, H.; Bin, L. Rapid prediction model for urban floods based on a light gradient boosting machine approach and hydrological–hydraulic model. *Int. J. Disaster Risk Sci.* **2023**, *14*, 79–97. [CrossRef]
243. Tanim, A.H.; McRae, C.B.; Tavakol-Davani, H.; Goharian, E. Flood detection in urban areas using satellite imagery and machine learning. *Water* **2022**, *14*, 1140. [CrossRef]
244. Composto, R.W.; Tulbure, M.G.; Tiwari, V.; Gaines, M.D.; Caineta, J. Quantifying urban flood extent using satellite imagery and machine learning. *Nat. Hazards* **2024**, *121*, 175–199. [CrossRef]
245. Mohamadiazar, N.; Ebrahimian, A.; Hosseiny, H. Integrating deep learning, satellite image processing, and spatial-temporal analysis for urban flood prediction. *J. Hydrol.* **2024**, *639*, 131508. [CrossRef]
246. Kundzewicz, Z.W.; Kanae, S.; Seneviratne, S.I.; Handmer, J.; Nicholls, N.; Peduzzi, P.; Mechler, R.; Bouwer, L.M.; Arnell, N.; Mach, K. Flood risk and climate change: Global and regional perspectives. *Hydrol. Sci. J.* **2014**, *59*, 1–28. [CrossRef]
247. Beniston, M.; Stoffel, M. Rain-on-snow events, floods and climate change in the Alps: Events may increase with warming up to 4 C and decrease thereafter. *Sci. Total Environ.* **2016**, *571*, 228–236. [CrossRef]
248. Rincón, D.; Khan, U.T.; Armenakis, C. Flood risk mapping using GIS and multi-criteria analysis: A greater Toronto area case study. *Geosciences* **2018**, *8*, 275. [CrossRef]
249. Terzi, S.; Torresan, S.; Schneiderbauer, S.; Critto, A.; Zebisch, M.; Marcomini, A. Multi-risk assessment in mountain regions: A review of modelling approaches for climate change adaptation. *J. Environ. Manag.* **2019**, *232*, 759–771. [CrossRef]
250. Wdowinski, S.; Bray, R.; Kirtman, B.P.; Wu, Z. Increasing flooding hazard in coastal communities due to rising sea level: Case study of Miami Beach, Florida. *Ocean Coast. Manag.* **2016**, *126*, 1–8. [CrossRef]
251. Li, C.; Xue, Y.; Fu, X. Urban Built Environment and Flood Ramifications: Evidence from Insurance Claims Data in Miami, Florida. *J. Plan. Educ. Res.* **2024**, 1–11. [CrossRef]
252. Brody, S.; Blessing, R.; Sebastian, A.; Bedient, P. Examining the impact of land use/land cover characteristics on flood losses. *J. Environ. Plan. Manag.* **2014**, *57*, 1252–1265. [CrossRef]
253. Zope, P.; Eldho, T.; Jothiprakash, V. Impacts of land use–land cover change and urbanization on flooding: A case study of Oshiwara River Basin in Mumbai, India. *Catena* **2016**, *145*, 142–154. [CrossRef]
254. Zhang, W.; Hu, B.; Liu, Y.; Zhang, X.; Li, Z. Urban Flood Risk Assessment through the Integration of Natural and Human Resilience Based on Machine Learning Models. *Remote Sens.* **2023**, *15*, 3678. [CrossRef]
255. Chen, G.; Hou, J.; Liu, Y.; Xue, S.; Wu, H.; Wang, T.; Lv, J.; Jing, J.; Yang, S. Urban inundation rapid prediction method based on multi-machine learning algorithm and rain pattern analysis. *J. Hydrol.* **2024**, *633*, 131059. [CrossRef]

256. Yang, H.; Zou, T.; Liu, B. Assessment of urban flood susceptibility based on a novel integrated machine learning method. *Environ. Monit. Assess.* **2025**, *197*, 25. [CrossRef]
257. Li, W.; Jiang, R.; Wu, H.; Xie, J.; Zhao, Y.; Li, F.; Gan, T.Y. An integrated urban flooding risk analysis framework leveraging machine learning models: A case study of Xi'an, China. *Int. J. Disaster Risk Reduct.* **2024**, *112*, 104770. [CrossRef]
258. Bosseler, B.; Salomon, M.; Schlüter, M.; Rubinato, M. Living with urban flooding: A continuous learning process for local municipalities and lessons learnt from the 2021 events in Germany. *Water* **2021**, *13*, 2769. [CrossRef]
259. Wang, H.; Meng, Y.; Xu, H.; Wang, H.; Guan, X.; Liu, Y.; Liu, M.; Wu, Z. Prediction of flood risk levels of urban flooded points though using machine learning with unbalanced data. *J. Hydrol.* **2024**, *630*, 130742. [CrossRef]
260. Costache, R.; Bui, D.T. Spatial prediction of flood potential using new ensembles of bivariate statistics and artificial intelligence: A case study at the Putna river catchment of Romania. *Sci. Total Environ.* **2019**, *691*, 1098–1118. [CrossRef]
261. Tehrany, M.S.; Pradhan, B.; Mansor, S.; Ahmad, N. Flood susceptibility assessment using GIS-based support vector machine model with different kernel types. *Catena* **2015**, *125*, 91–101. [CrossRef]
262. Liang, Z.; Wang, C.-M.; Zhang, Z.-M.; Khan, K.-U.-J. A comparison of statistical and machine learning methods for debris flow susceptibility mapping. *Stoch. Environ. Res. Risk Assess.* **2020**, *34*, 1887–1907. [CrossRef]
263. Wang, Y.; Sun, D.; Wen, H.; Zhang, H.; Zhang, F. Comparison of random forest model and frequency ratio model for landslide susceptibility mapping (LSM) in Yunyang County (Chongqing, China). *Int. J. Environ. Res. Public Health* **2020**, *17*, 4206. [CrossRef] [PubMed]
264. Elmahdy, S.I.; Mohamed, M.M.; Ali, T.A.; Abdalla, J.E.-D.; Abouleish, M. Land subsidence and sinkholes susceptibility mapping and analysis using random forest and frequency ratio models in Al Ain, UAE. *Geocarto Int.* **2022**, *37*, 315–331. [CrossRef]
265. Bowei, Z.; Huang, G.; Wenjie, C. Research progress and prospects of urban flooding simulation: From traditional numerical models to deep learning approaches. *Environ. Model. Softw.* **2024**, *183*, 106213.
266. Lei, X.; Chen, W.; Panahi, M.; Falah, F.; Rahmati, O.; Uuemaa, E.; Kalantari, Z.; Ferreira, C.S.S.; Rezaie, F.; Tiefenbacher, J.P. Urban flood modeling using deep-learning approaches in Seoul, South Korea. *J. Hydrol.* **2021**, *601*, 126684. [CrossRef]
267. Shao, Y.; Chen, J.; Zhang, T.; Yu, T.; Chu, S. Advancing rapid urban flood prediction: A spatiotemporal deep learning approach with uneven rainfall and attention mechanism. *J. Hydroinform.* **2024**, *26*, 1409–1424. [CrossRef]
268. Zhong, P.; Liu, Y.; Zheng, H.; Zhao, J. Detection of urban flood inundation from traffic images using deep learning methods. *Water Resour. Manag.* **2024**, *38*, 287–301. [CrossRef]
269. Moon, H.; Yoon, S.; Moon, Y. Urban flood forecasting using a hybrid modeling approach based on a deep learning technique. *J. Hydroinform.* **2023**, *25*, 593–610. [CrossRef]
270. Youssef, A.M.; Pourghasemi, H.R.; Mahdi, A.M.; Matar, S.S. Flood vulnerability mapping and urban sprawl suitability using FR, LR, and SVM models. *Environ. Sci. Pollut. Res.* **2023**, *30*, 16081–16105. [CrossRef]
271. Liu, K.; Kinouchi, T.; Tan, R.; Heng, S.; Chhuon, K.; Zhao, W. Unraveling urban hydro-environmental response to climate change and MCDA-based area prioritization in a data-scarce developing city. *Sci. Total Environ.* **2024**, *948*, 174389. [CrossRef]
272. Akay, H. Flood hazards susceptibility mapping using statistical, fuzzy logic, and MCDM methods. *Soft Comput.* **2021**, *25*, 9325–9346. [CrossRef]
273. Madhuri, R.; Sistla, S.; Srinivasa Raju, K. Application of machine learning algorithms for flood susceptibility assessment and risk management. *J. Water Clim. Change* **2021**, *12*, 2608–2623. [CrossRef]
274. Hasanuzzaman, M.; Islam, A.; Bera, B.; Shit, P.K. A comparison of performance measures of three machine learning algorithms for flood susceptibility mapping of river Silabati (tropical river, India). *Phys. Chem. Earth Parts A/B/C* **2022**, *127*, 103198. [CrossRef]
275. Das, S. Geospatial mapping of flood susceptibility and hydro-geomorphic response to the floods in Ulhas basin, India. *Remote Sens. Appl. Soc. Environ.* **2019**, *14*, 60–74. [CrossRef]
276. Das, S. Flood susceptibility mapping of the Western Ghat coastal belt using multi-source geospatial data and analytical hierarchy process (AHP). *Remote Sens. Appl. Soc. Environ.* **2020**, *20*, 100379. [CrossRef]
277. Rahman, M.; Ningsheng, C.; Mahmud, G.I.; Islam, M.; Pourghasemi, H.; Ahmad, H.; Habumugisha, J.; Washakh, R.; Alam, M.; Liu, E. Flooding and its relationship with land cover change, population growth, and road density. *Geosci. Front.* **2021**, *12*, 101224. [CrossRef]